Comments on Inorganic Chemistry
Publication details, including instructions for authors and subscription information:
http://www.informaworld.com/smpp/title~content=t713455155

COORDINATION AND BIOINORGANIC CHEMISTRY OF ARYL-APPENDED TRIS(2-PYRIDYLMETHYL)AMINE LIGANDS

Lisa M. Berreau[a]
[a] Department of Chemistry & Biochemistry, Utah State University, Logan, Utah, USA

To cite this Article Berreau, Lisa M.(2007) 'COORDINATION AND BIOINORGANIC CHEMISTRY OF ARYL-APPENDED TRIS(2-PYRIDYLMETHYL)AMINE LIGANDS', Comments on Inorganic Chemistry, 28: 3, 123 — 171
To link to this Article: DOI: 10.1080/02603590701572940
URL: http://dx.doi.org/10.1080/02603590701572940

Comments on Inorganic Chemistry, 28: 123–171, 2007

ISSN: 0260-3594 print
DOI: 10.1080/02603590701572940

Taylor & Francis
Taylor & Francis Group

COORDINATION AND BIOINORGANIC CHEMISTRY OF ARYL-APPENDED TRIS(2-PYRIDYLMETHYL)AMINE LIGANDS

LISA M. BERREAU

Department of Chemistry & Biochemistry, Utah State University, Logan, Utah, USA

Aryl-appended tris(2-pyridylmethyl)amine ligands are a relatively new class of chelate ligands in coordination and synthetic bioinorganic chemistry. As outlined herein, to date, coordination complexes of such ligands have been prepared and characterized for first row metal ions from groups 7–12. These studies revealed key coordination properties for this family of ligands. Aryl-appended tris(2-pyridylmethyl)amine ligands have been recently employed in synthetic, biologically relevant metal complexes that exhibit: 1) arene hydroxylation reactivity relevant to non-heme iron-containing containing enzymes that hydroxylate aromatic amino acids; and 2) structural and reactivity properties relevant to Ni(II)-containing acireductone dioxygenase, urease, and glyoxalase I enzymes.

***Keywords*: carboxylate shift, cobalt, copper, iron, manganese, nickel, nitrogen ligands, oxygen activation, zinc**

INTRODUCTION

Efforts toward designing new ligands are increasingly focused on influencing both the primary and secondary coordination environment of the metal center. This is particularly true in the area of synthetic bioinorganic chemistry where biomimetic and bioinspired complexes are sought to further understand and/or mimic the reactivity features of biological

Address correspondence to Lisa M. Berreau, Department of Chemistry & Biochemistry, Utah State University, Logan, UT 84322-0300, USA. E-mail: berreau@cc.usu.edu

metal centers. Tris(2-pyridylmethyl)amine (TPA) ligands have been widely employed in modeling the structural and functional aspects of the active site metal centers in metalloenzymes.[1] In recent years, hydrogen bond donor appended TPA ligands have been used to isolate novel mononuclear 3*d* metal aqua, hydroxide, methoxide, phenoxide, hydroperoxide, and alkylperoxide complexes.[2–17] From these investigations, significant insight has been gained into how secondary hydrogen bonding interactions can be used to stabilize reactive metal-bound ligands.

Studies of the influence of a hydrophobic secondary environment on the chemistry of biologically relevant metal complexes are currently fewer in number. In terms of enzymatic studies, the presence of active site hydrophobic amino acid residues has been suggested to influence properties of the metal center including its redox potential[18] and the orientation of a coordinated substrate.

In this contribution, I outline how over the past ~12 years aryl-appended TPA ligands have been developed and used to construct interesting coordination compounds, some of which exhibit structural, spectroscopic, and reactivity properties of relevance to biological metal centers. This review/commentary is presented in four sections. First, synthetic routes for the preparation of aryl-appended TPA ligands are described. Second, the scope of the general coordination chemistry of these ligands for metal ions of groups 7–12 is presented. This portion includes an emphasis on structural and spectroscopic features characteristic of complexes of this ligand class. In the third section, the structural and reactivity properties of biologically relevant complexes of aryl-appended TPA ligands are described. The final section addresses the impact of the work presented in the first three sections and discusses the outlook for further research using these ligands.

SYNTHESIS OF ARYL-APPENDED TRIS(2-PYRIDYLMETHYL)-AMINE LIGANDS

Attachment of a 2-aryl group to a pyridyl ring is easily achieved via a Suzuki coupling reaction involving a bromopyridyl precursor and a boronic acid containing the appropriate aryl group. This reaction may be performed using a single pyridyl unit (e.g. 6-bromopicolylaldehyde[19]; Scheme 1(a)) or a tris(2-pyridylmethyl)amine ligand having a 6-bromo substituent[20] (Scheme 1(b,c)). The yield of the former reaction for the bromopyridine carboxaldehyde is 65–90% after purification of the

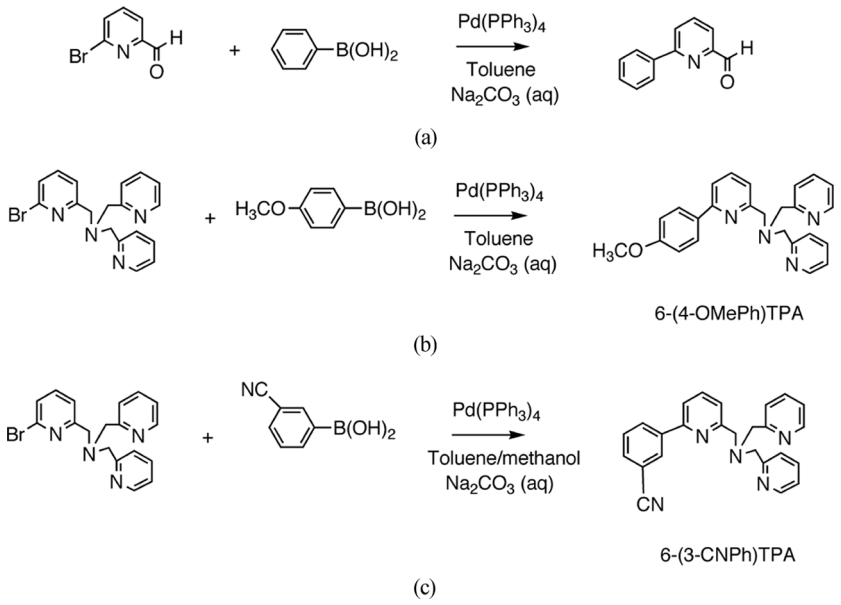

Scheme 1. Suzuki coupling reactions used to produce aryl-appended pyridyl derivatives and ligands.

product by column chromatography.[21] Several aryl-appended pyridinecarboxaldehydes (3,5-(dimethyl)phenyl, 3-(nitro)phenyl, 3-(trifluoromethyl)phenyl, 3-(chloro)phenyl, 3-(methyl)phenyl, 3-(methoxy)phenyl, and 4-methoxy-(phenyl), and 2,3-dihydroxo(phenyl) have been prepared using this procedure starting from the appropriate boronic acid.[22,23] The latter reaction has thus far only been used for the preparation of 6-(4-OMePh)TPA, 6-(3-CNPh)TPA, BCATTPA, and α-$MePh_2$TPA (Figure 1).[24–26] A procedure for the preparation of *o*-d_1-6-phenyl-2-pyridinecarboxaldehyde has also been reported.[23]

To construct an aryl-appended tris(2-pyridylmethyl)amine (TPA) ligand starting from the aryl-appended carboxaldehyde, a common synthetic pathway involves (1) reduction of the aldehyde group using $NaCNBH_3$[27] or $NaBH_4$[28] to generate a primary alcohol, (2) treatment of this alcohol with $SOCl_2$[21,22,27] or PBr_3[28] to generate a 2-halomethyl intermediate, and (3) heating of this intermediate with a 2-(aminomethyl)pyridine derivative in the presence of base to produce a mono-, di- or triaryl-appended chelate ligand. An alternative synthetic route

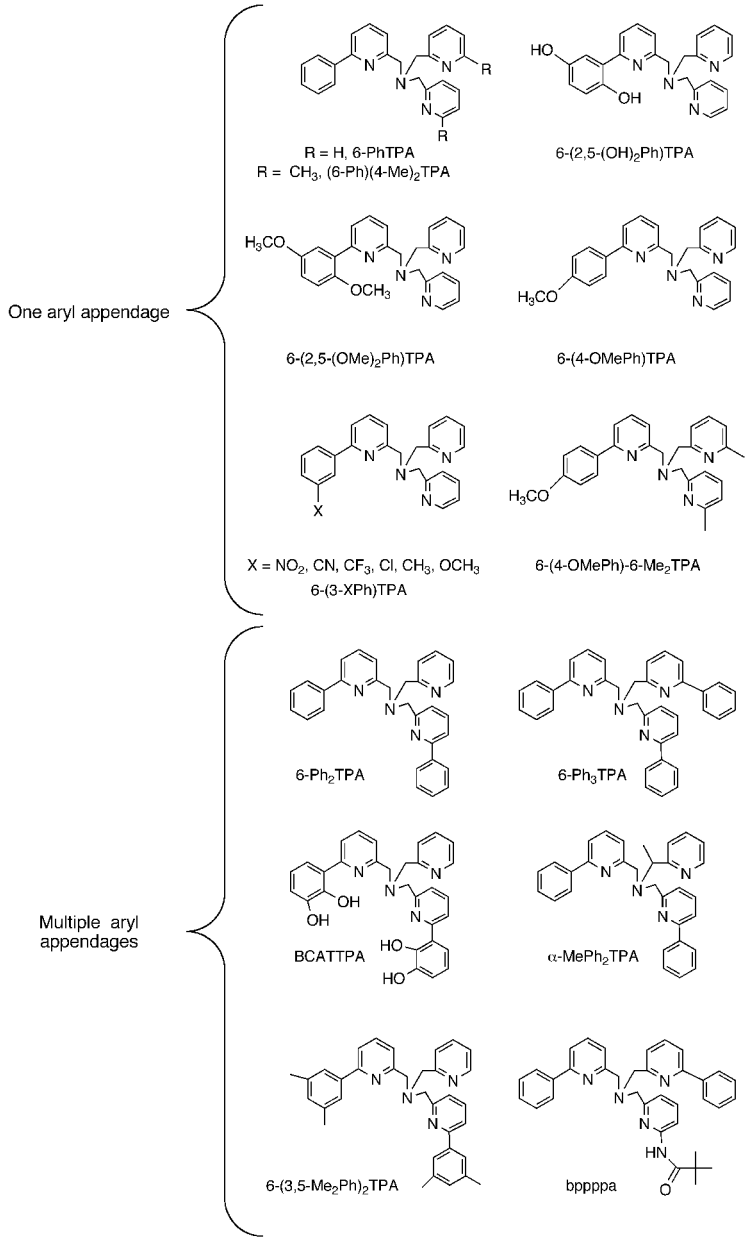

Figure 1. Aryl-appended TPA ligands.

involves reductive amination via treatment of the aryl-appended pyridine carboxaldehyde with a 2-(aminomethyl)pyridine derivative in the presence of $NaCNBH_3$.[23,27–29] The amide-appended ligand bppppa was prepared via an alkylation pathway involving *N*,*N*-bis((6-phenyl-2-pyridyl)methyl)amine and 2-bromomethyl-6-pivaloylamidopyridine.[30,31] All aryl-appended TPA ligands reported to date that have been used to generate structurally characterized metal complexes are shown in Figure 1.

Ligands having two aryl-linked tris(2-pyridylmethyl)amine motifs have been reported.[32] However, no further discussion of these ligands is presented in this contribution. Tripodal tetradentate ligands having one or two aryl-appended pyridyl groups and a N_3O-donor set, which includes a deprotonated phenol, have been employed for the preparation of a family of Zn(II) complexes.[33] Due to the heterogeneity of the donor set, these ligands are not included in this review/commentary.

COORDINATION CHEMISTRY: STRUCTURAL, MAGNETIC, AND SPECTROSCOPIC PROPERTIES OF METAL COMPLEXES OF ARYL-APPENDED TRIS(2-PYRIDYLMETHYL)AMINE LIGANDS

Aryl-appended TPA ligands have been used in the preparation of coordination complexes of Mn(II),[22,28] Fe(II) and Fe(III),[20,23–25,28,34,35] Co(II),[22,28,31] Ni(II),[22,28,31,36] Cu(I) and Cu(II),[21,27,28,37–39] and Zn(II).[22,28,31]

Mn(II). One Mn(II) complex of the 6-(2,5-$(OMe)_2$Ph)TPA ligand, [(6-(2,5-$(OMe)_2$Ph)TPA)$MnCl_2$] (**1**), and two divalent manganese complexes of the 6-Ph_2TPA ligand, [(6-Ph_2TPA)$Mn(CH_3OH)_3](ClO_4)_2$ (**2**) and [(6-Ph_2TPA$Mn)_2(\mu$-$ONHC(O)CH_3)_2](ClO_4)_2$ (**3**), have been prepared and structurally characterized.[22,28] Two crystalline forms of **2** (**A** and **B**) were produced. These differ in the number of nonocoordinated methanol molecules found in the lattice (**A**: CH_3OH; **B**: 2 CH_3OH). Drawings of **1**–**3** are shown in Figure 2. The Mn(II) center(s) in each complex are six-coordinate with a distorted octahedral geometry. In **1**, the chelate ligand coordinates to Mn(II) via all four nitrogen donors whereas in the 6-Ph_2TPA complexes, each Mn(II) center adopts a distorted octahedral geometry, with only one of the two phenyl-appended pyridyl appendages of the ligand coordinated to the Mn(II) center. In **2**, the three nitrogen donors of the 6-Ph_2TPA ligand are coordinated in a meridional fashion, whereas in **3** these donors are bound in a facial array.

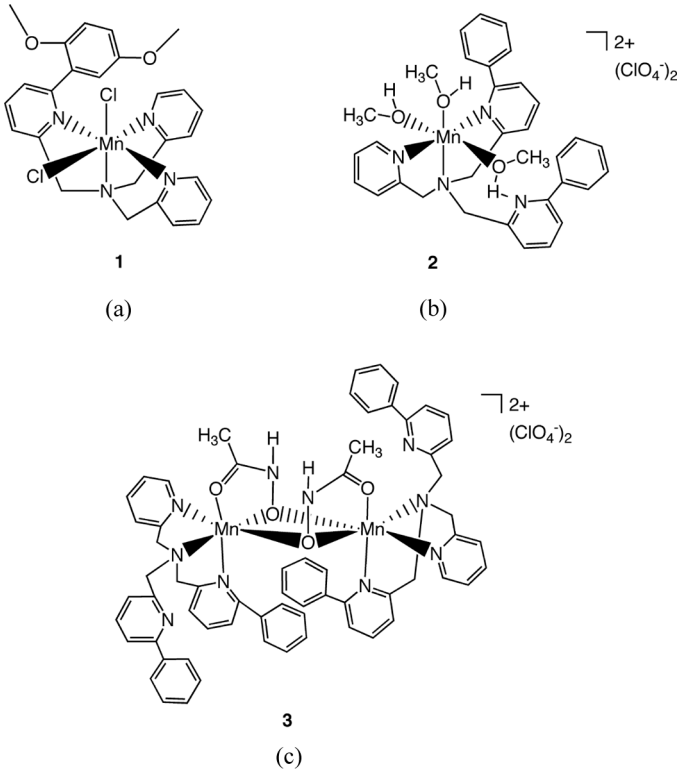

Figure 2. Drawings of the Mn(II) complexes **1**–**3**.

In **2**, the noncoordinated phenyl-appended pyridyl moiety acts as a hydrogen bond acceptor for a Mn(II)-coordinated methanol ligand. Another coordinated methanol participates in a CH/π interaction[40,41] with a phenyl appendage of the chelate ligand. Evidence for this interaction is a short C(methanol)–arene centroid distance ($\sim$3.4 Å). This type of interaction provides a small amount of stabilization energy ($<$8 kJ/mol) to the Mn(II)-coordinated methanol molecule.[41] The hydroxamate ligands of **3** are each coordinated in a μ-η^1:η^2 fashion. One relatively weak hydrogen bond is found between a hydroxamate N-H and a nitrogen atom (N(4)) of one noncoordinated phenyl-appended pyridyl moiety.

Complexes **1**–**3** all contain high spin Mn(II) centers, albeit the magnetic moment for **3** ($\mu_{eff} = 5.6\,\mu_B$/Mn(II)) is slightly lower than the

spin-only magnetic moment for isolated Mn(II) ($\mu_{eff} = 5.9\,\mu_B$/Mn(II)) centers.[42]

Fe(II). Eight Fe(II) complexes of aryl-appended TPA ligands have been reported.[23,25,28,34] Drawings of these complexes are shown in Figures 3 and 4. Three of the mononuclear Fe(II) complexes supported by a monoaryl-appended TPA ligand, [(6-PhTPA)Fe$(CH_3CN)_2$]-$(ClO_4)_2$[23,35] (**4**, Figure 3(a)), [(6-(3-OMePh)TPA)Fe$(OTf)_2$][23] (**5**, Figure 3(b)), and [(6-(2,5-OMe_2Ph)TPA)$FeCl_2$][28] (**7**, Figure 3(c)), exhibit tetradentate coordination of the chelate ligand, an overall coordination number of six, and a distorted octahedral geometry. The structure of [((6-Ph)(4-$Me)_2$TPA)Fe$(OTf)_2]_2$[23] (**6**, Figure 4) is notably different, with tridentate, meridional coordination of the chelate ligand to each Fe(II) center in the binuclear structure. This complex contains two bridging triflate anions and a terminal triflate on each Fe(II) center. The cyano-appended ligand 6-(3-CNPh)TPA yields a distorted square pyramidal ($\tau = 0.09$)[43] iron dichloride complex (**8**, Figure 3(d)) having a tridentate, meridional chelate ligand and a noncoordinated aryl-appended pyridyl donor. Treatment of **8** with $FeCl_2$ yields [((6-(3-CNPh)TPA)$Fe)_2$-$(\mu$-$Cl)_2]FeCl_4$ (**9**, Figure 3(e)), which contains a binuclear bis(μ-chloro) diferrous cation wherein each chelate ligand is coordinated in a tetradentate fashion. One Fe(II) complex of the 6-Ph_2TPA ligand, [(6-Ph_2TPA)-$FeCl_2$] (**10**, Figure 3(f)), has been reported.[34] The Fe(II) center in this complex has a distorted square pyramidal geometry ($\tau = 0.33$)[43] and tridentate coordination of the 6-Ph_2TPA ligand, with one dangling phenyl-appended pyridyl appendage.

Complexes **4–10** each contain one or two high-spin ($S = 2$) Fe(II) centers. Despite their paramagnetic character, such complexes are amenable to characterization by ^{1}H NMR. The spectra of **4–6** in CD_3CN are consistent with the presence of a $[(L)Fe(NCCD_3)_2]^{2+}$ cation in solution wherein all four donors of the chelate ligand are coordinated to the Fe(II) center.[23] Broad resonances are found in the chemical shift range of $\sim+110$ to -10 ppm for **4** and **5**, and $\sim+125$ to -30 ppm for **6**. The shifts of these resonances are primarily due to σ-spin delocalization effects, indicating that the closer a hydrogen atom is to the paramagnetic Fe(II) center, the greater the chemical shift of the hydrogen atom resonance. Assignment of β/β' and γ/γ' resonances (Figure 5) was made on the basis of signal intensity and ^{1}H-^{1}H COSY spectra. The identification of a 2:1 intensity pattern for the β/β' and γ/γ' signals in **4–6** is consistent with an effective mirror plane that bisects the two unsubstituted pyridyl

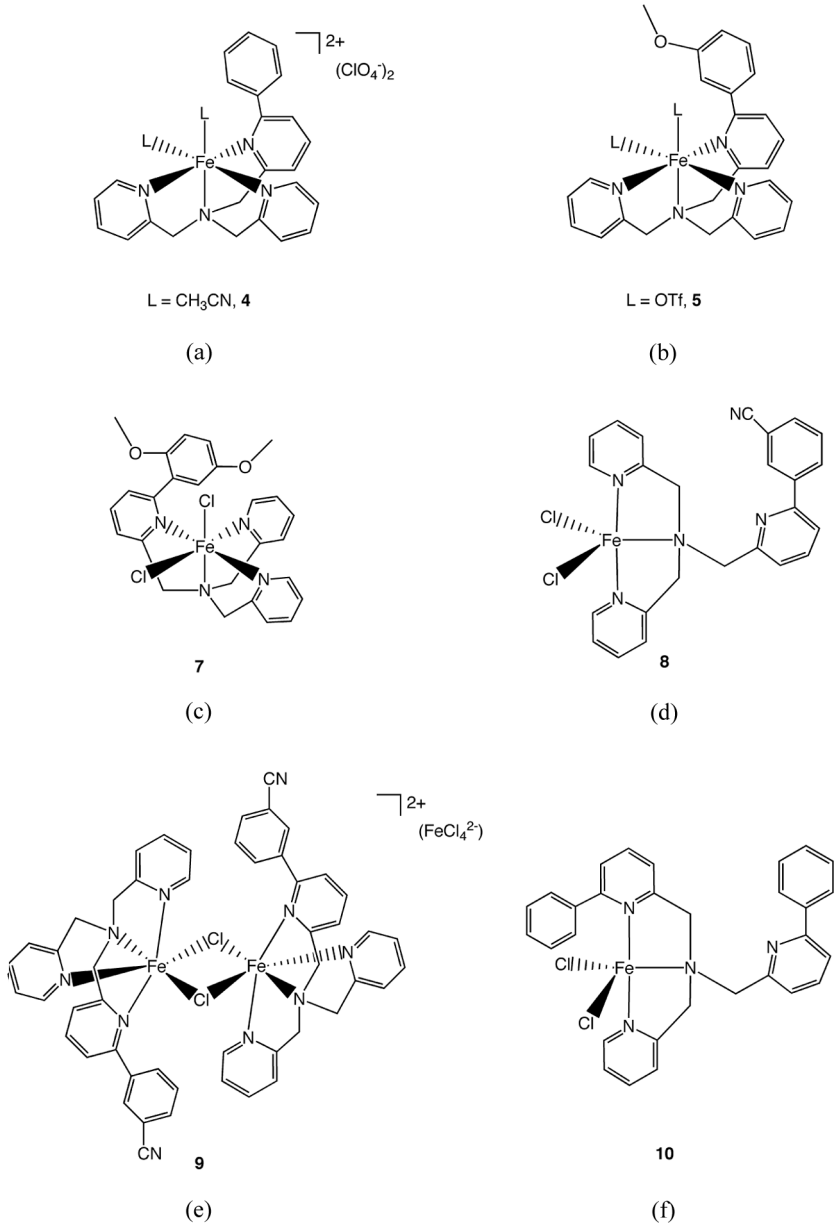

Figure 3. Drawings of the Fe(II) complexes **4**, **5**, and **7**–**10**.

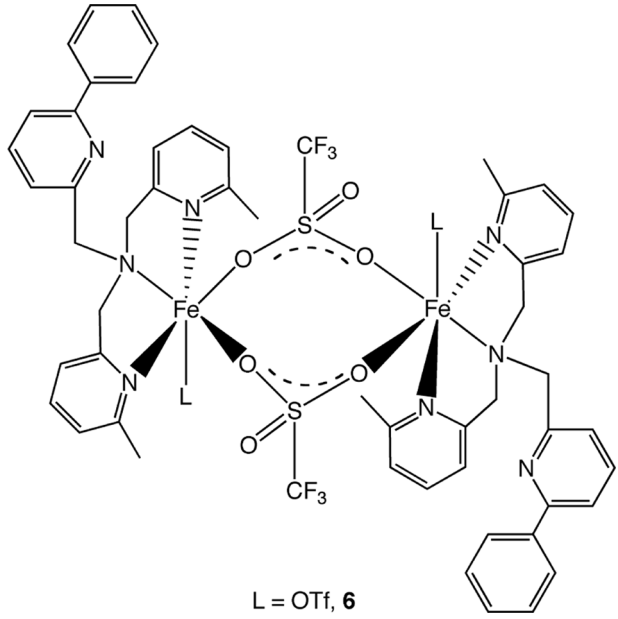

Figure 4. Drawing of the Fe(II) complex **6**.

donors. This requires a rapid rearrangement of the unsymmetric chelate ligand environment of the cation in solution. The phenyl ring protons of **4** and **5** are shifted slightly upfield ($\sim$2.3 to $-$0.8 ppm) whereas those in **6** are essentially unshifted.

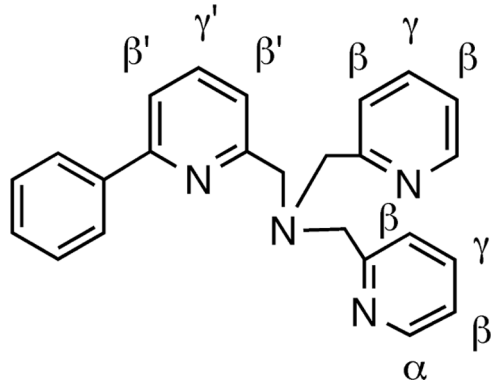

Figure 5. Labeling scheme for a 6-PhTPA-type ligand.

^{1}H NMR spectroscopic data has not been reported for complex **7**.[28] However, data has been reported for [(6-(3-CNPh)TPA)$FeCl_2$] (**8**), [((6-(3-CNPh)TPA)Fe)$_2$(μ-Cl)$_2$]$FeCl_4$ (**9**), and [(6-Ph_2TPA)$FeCl_2$] (**10**).[25,34] For **8**, resonances are found in the chemical shift range of $\delta \sim 130$ to ~ 10 ppm. The β/β' resonances of **8** are found in the region of ~ 55 to 25 ppm, whereas in **9** these signals are shifted downfield slightly and are found in the range of ~ 60 to 35 ppm. Using a d^{10} analog of **10** ([(6-(d_5-Ph)$_2$TPA)$FeCl_2$]) one set of phenyl protons was identified using ^{2}H NMR. This indicates only one phenyl-appended pyridyl environment in the solution structure of **10** and coordination of both phenyl-appended pyridyl donors (at least transiently) to the Fe(II) center. Consistent with this analysis is the identification of only two γ/γ' (Figure 6) resonances at 7.5 and 4.5 ppm.

An Fe(II) complex of the BCATTPA ligand, [(HBCATTPA)$FeCl_2$] (**11**, Figure 7) having tridentate coordination of the chelate ligand, has been recently reported.[24] Its structure has been proposed on the basis of spectroscopic data (^{1}H NMR, UV-vis). In this complex, one deprotonated hydroxyl group of the aryl appendage is coordinated to the Fe(II) center and the noncoordinated pyridyl nitrogen is protonated. When dissolved in CD_3CN, this complex exhibits resonances in the chemical shift range of $\sim +130$ to -10 ppm.

When dissolved in propionitrile, **4** and **5** exhibit absorption features at ~ 360 and ~ 400 nm, respectively, which are assigned to Fe(II) $\rightarrow$ N(py) MLCT transitions.[23] The intensity of these features increases with decreasing temperature, which is consistent with spin crossover of the Fe(II) center from an $S = 2$ to an $S = 0$ spin state.[44–47] Complex **6** does not exhibit such behavior, consistent with a weaker ligand field for the (6-Ph)(4-Me)$_2$TPA

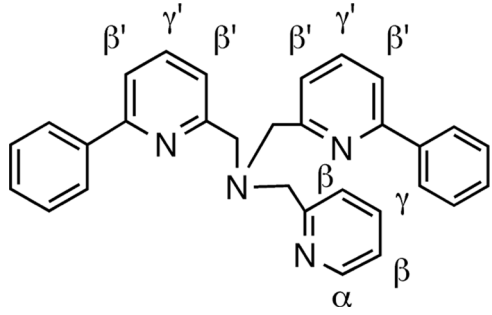

Figure 6. Labeling scheme for a (6-Ph)$_2$TPA ligand.

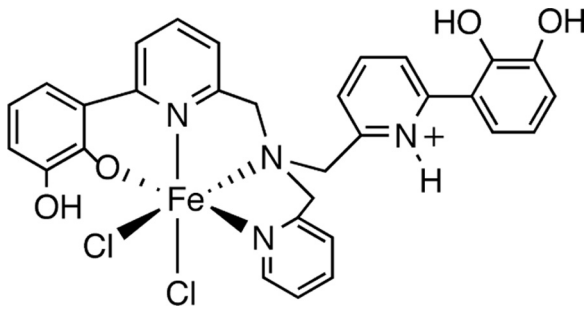

Figure 7. Proposed structure of [(HBCATTPA)$FeCl_2$] (**11**).

chelate ligand.[23] The UV-vis spectrum of [(HBCATTPA)$FeCl_2$] (**9**, Figure 7) in acetonitrile contains two absorption features at 355 ($\varepsilon = 2980\,M^{-1}cm^{-1}$) and 446 ($\varepsilon = 720\,M^{-1}cm^{-1}$) nm, respectively. The former was assigned as a phenolate → Fe(II) LMCT transition and the latter as an Fe(II) → N(py) MLCT transition for the chelate ligand coordinated in a κ^3 coordination mode.[24,34]

Fe(III). Drawings of three structurally characterized examples of Fe(III) chloride complexes of aryl-appended TPA ligands are shown in Figure 8.[20,24] Complexes **11** ([6-(4-OMePh)TPA)$FeCl_3$], Figure 8(a)), and **12** ([(BCATTPA)$FeCl_2$], Figure 8(b)), both contain a distorted octahedral Fe(III) center. In **11** the aryl-appended chelate ligand is coordinated in a facial N_3-donor, κ^3-type manner with chloride anions filling the three remaining metal coordination sites. Tetradentate coordination is found with the BCATTPA ligand in **12**, with three coordinated nitrogen donors and one deprotonated hydroxyl oxygen atom. One of the catechol-appended pyridyl groups of the BCATTPA ligand is not coordinated.

The diiron catecholate complex [(BCATTPA)Fe_2Cl_2] (**13**, Figure 8(c)) is the product of the reaction of [(HBCATTPA)$FeCl_2$] (**11**, Figure 7) with O_2 in CH_3CN or THF.[24] One iron center exhibits a coordination number of seven, with κ^4-coordination of the four nitrogen donors of the BCATTPA ligand. This iron center is also coordinated to two bridging phenolate oxygen atoms and one terminal chloride ligand. The other iron center exhibits a coordination number of five and a distorted square pyramidal geometry. Notably, the formation of **13** from the reaction of **9** with O_2 requires the decomplexation of one BCATTPA chelate ligand to enable the generation of free Fe(III) ion.

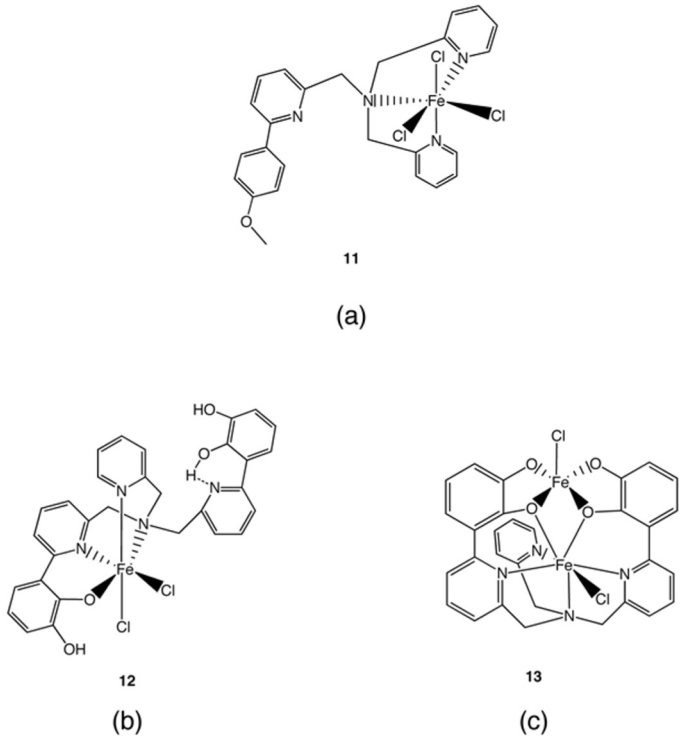

Figure 8. Drawings of the Fe(III) complexes **11–13**.

The ^{1}H NMR spectrum of **11** in CD_3CN contains multiple resonances in the chemical shift range of $\sim+110$ to 0 ppm.[20] Initial assignment of these resonances was made on the basis of integrated intensity and T_1 values. For **12**, only two broad ^{1}H NMR resonances could be identified at $\delta = 95$ and 60 ppm.[24] The UV-vis spectrum of **11** contains an absorbance at 385 nm ($\varepsilon = 3690\,M^{-1}cm^{-1}$) which is assigned as a chloride to Fe(III) LMCT transition.[34] A similar transition is found at 354 nm in the UV-vis spectrum of **12**.[24] Phenolate coordination in this complex is indicated by the presence of a phenolate $\rightarrow$ Fe(III) LMCT transition at 617 nm ($\varepsilon = 820\,M^{-1}cm^{-1}$).

No paramagnetically shifted resonances were detected in the ^{1}H NMR spectrum of **13**. A magnetic moment has not been reported for this complex. The UV-vis spectrum of **13** contains a phenolate $\rightarrow$ Fe(III) LMCT transition at 590 nm (1100 $M^{-1}cm^{-1}$).[24]

Co(II). Four mononuclear Co(II) complexes (**14–17**) of aryl-appended TPA ligands have been reported.[22,28,31] All have been characterized by X-ray crystallography and drawings of these complexes are shown in Figure 9. Three of these complexes [(6-(2,5-$(OMe)_2$Ph)TPA)CoCl]BPh_4 (**14**), [(6-Ph_2TPA)Co(CH_3CN)]$(ClO_4)_2$ (**15**), and [(bppppa)Co]$(ClO_4)_2$ (**17**)) have a Co(II) center having a coordination number of five, a distorted trigonal bipyramidal geometry (**14**: $\tau = 0.92$; **15**: $\tau = 0.84$; **17**: $\tau = 0.67$), and the pyridyl donors in the pseudo equatorial plane.[43] In each of these complexes, the Co-N distances involving the aryl-appended pyridyl donors are slightly longer ($\sim$0.02–0.06 Å) than the Co-N_{py} distance. The methyl group of the coordinated acetonitrile ligand in **15** participates in secondary CH/π interactions[41] with both phenyl groups of the 6-Ph_2TPA ligand. These interactions, which involve C(methyl)...arene centroid distances of 3.79 and 3.80 Å, are longer than the CH/π interaction in the Mn(II) complex [(6-Ph_2TPA)Mn(CH_3OH)$_3$]$(ClO_4)_2$ (**2**), which has a C(methyl)...arene centroid distance of $\sim$3.4 Å.[22]

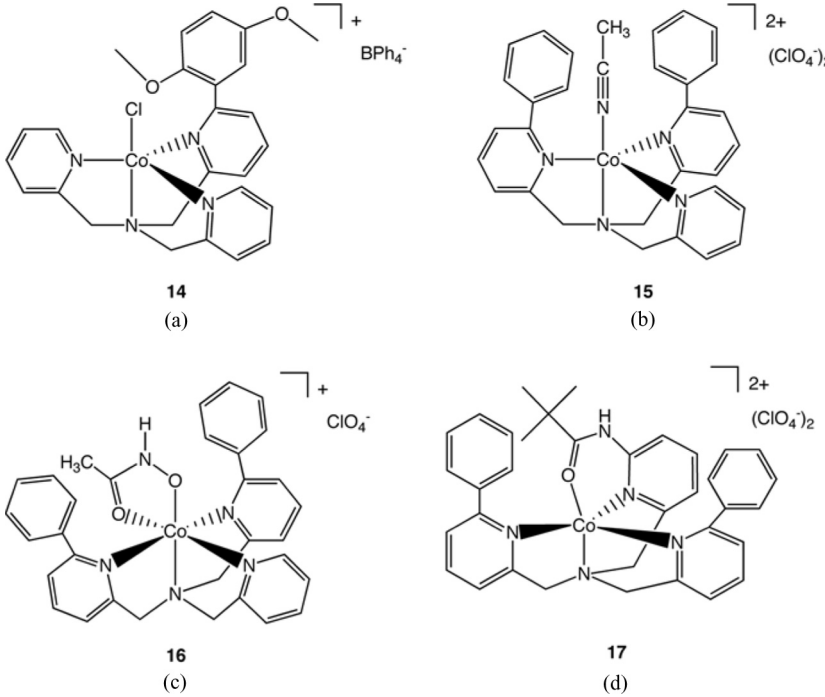

Figure 9. Drawings of the Co(II) complexes **14–17**.

The hydroxamate complex $[(6\text{-}Ph_2TPA)Co(ONHC(O)CH_3)]ClO_4$ (**16**, Figure 9(c)) has a Co(II) center having a coordination number of six and a distorted octahedral geometry. The hydroxamate ligand is positioned in a sandwich-type motif between the two aryl appendages of the $6\text{-}Ph_2TPA$ chelate ligand. The $Co\text{-}N_{PhPy}$ distances are ~ 0.15 Å longer than the $Co\text{-}N_{Py}$ distance.

The Co(II) complexes **14** (Figure 9(a)) and **15** (Figure 9(b)) have been characterized by a magnetic moment measurement. A solid sample of **14** was found to exhibit a magnetic moment of $4.70\,\mu_B$ as measured using a Guoy balance.[28] The magnetic moment of **15** ($\mu_{eff} = 4.3\,\mu_B$) was measured using the solution Evans method.[22] Both values are higher than the spin-only magnetic moment for a high-spin Co(II) ion ($3.9\,\mu_B$) due to spin-orbit coupling.[48] Similarly, the magnetic moment of **16**, measured using the Evans method, was determined to be $4.4\,\mu_B$.[22]

The UV-vis spectra of **14**, **15**, and **17** (Figure 9(d)) contain the three expected *d-d* absorption bands for a high-spin pseudo-trigonal bipyramidal Co(II) center.[49] For each complex, the molar absorptivity values for these absorbances are consistent with the Co(II) center retaining an overall coordination number of five in solution. Complex **16** (Figure 9(c)) exhibits three absorption features at 472 ($\varepsilon = 110\,M^{-1}cm^{-1}$), 562 ($\varepsilon = 30\,M^{-1}cm^{-1}$), and 925 nm ($\varepsilon = 6\,M^{-1}cm^{-1}$). The lower molar absorptivity of the 562 nm absorption band, as compared to a ~ 570 nm ($\varepsilon = 90\,M^{-1}cm^{-1}$) absorption feature in the UV-vis spectrum of **15**, is consistent with an increase in the coordination number of the Co(II) center in the hydroxamate complex.[22]

To date, ^1H NMR spectroscopic data has been reported for only one of the Co(II) complexes shown in Figure 9. This complex, the amide-containing **17**, exhibits signals over a chemical shift range of ~ 90 ppm.[31] The β' resonances (Figure 6) of the phenyl-appended pyridyl rings are found at 74.9 and 35.2 ppm in CD_3CN at 25(1)°C. These signals are coupled to a γ'-H resonance at 0.26 ppm, as determined by a ^1H–^1H COSY experiment. The *t*-butyl methyl resonance appears at 13.8 ppm, whereas that amide N-H resonance is found at -15.6 ppm. The assignment of the N-H resonance was confirmed via treatment of **16** with D_2O in CD_3CN, which resulted in the disappearance of the -15.6 ppm resonance.

Ni(II). Drawings of four structurally characterized mononuclear Ni(II) complexes of aryl-appended TPA ligands are shown in Figure 10 ((a)–(d)).[22,31,36] These complexes, $[(6\text{-}Ph_2TPA)Ni(CH_3CN)(CH_3OH)]$-

$(ClO_4)_2$ (**18**), $[(6\text{-}Ph_2TPA)Ni\text{–}Cl(CH_3CN)]ClO_4$ (**19**), $[(6\text{-}Ph_2TPA)Ni(ONHC(O)CH_3)]ClO_4$ (**20**), and $[(bppppa)Ni](ClO_4)_2$ (**21**), are all supported by a chelate ligand containing at least two phenyl-appended pyridyl donors. A binuclear Ni(II) chloride complex of the 6-(2,5-OMe_2Ph)TPA has also been reported.[28] A drawing of this complex, $[(6\text{-}(2,5\text{-}OMe_2Ph)TPANi)_2(\mu\text{-}Cl)_2]Cl_2$ (**22**), is shown in Figure 11.

In **18**–**20** the Ni(II) center exhibits a pseudo-octahedral geometry and κ^4 coordination of the aryl-appended TPA ligand. The Ni-N_{PhPy} distances in these complexes are $\geq$0.12 Å longer than the Ni-N_{Py} distance in each complex. It is worth noting that the orientation of hydroxamate coordination in **20** is reversed with respect to that found in $[(6\text{-}Ph_2TPA)Co(ONHC(O)CH_3)]ClO_4$ (**16**, Figure 9(c)). Specifically, in **20** the neutral carbonyl oxygen donor of the hydroxamate ligand is positioned *trans* to the tertiary amine nitrogen of the 6-Ph_2TPA ligand. This enables the formation of hydrogen-bonded pairs of dimers in the solid-state structure of **20** wherein the hydroxamate N-H moiety of one cation participates in a hydrogen bond with the coordinated deprotonated hydroxamate oxygen of another cation.

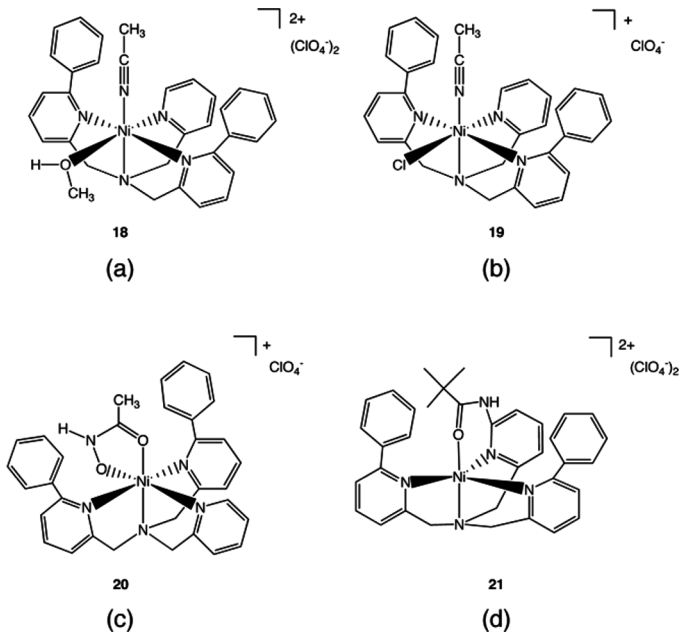

Figure 10. Drawings of the Ni(II) complexes **18**–**21**.

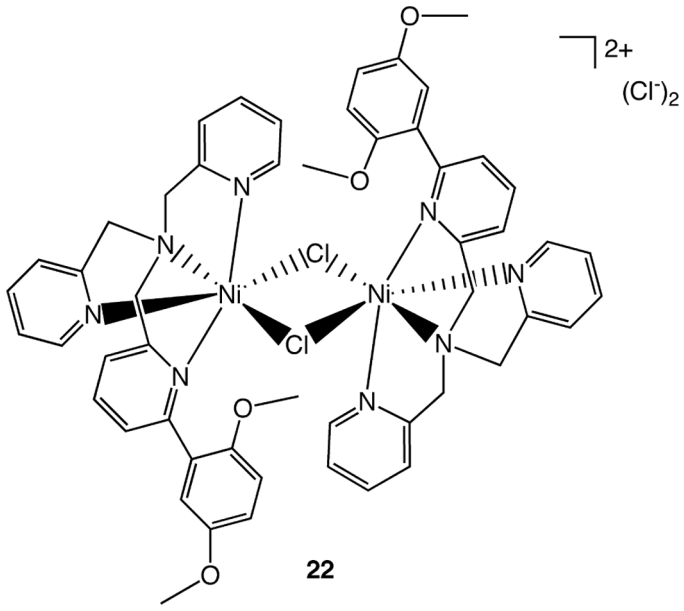

Figure 11. Drawing of the Ni(II) chloride complex **22**.

Complex **21** (Figure 10(d)) contains a Ni(II) center having a coordination number of five, with all donors coming from the bppppa chelate ligand, and a weak sixth interaction (Ni(1)...O(7) 2.975 Å) involving an oxygen atom of a perchlorate anion.[31] Consistent with the lower coordination number, the Ni-N_{PhPy} distances in **20** (Ni(1)–N(4) 2.0767(15); Ni(1)–N(5) 2.1051(15) Å) are notably shorter than average Ni-N_{PhPy} distance in **18** (2.21 Å), **19** (2.25 Å), and **20** (2.24 Å). The *tert*-butyl methyl substituent forms weak CH/π interactions (C(methyl)...arene centroid 3.95 and 3.80 Å) with the phenyl appendages of the bppppa ligand.[41]

In **22** (Figure 11), the Ni(II) centers are bridged in an asymmetric fashion by two chloride anions, with a Ni...Ni distance of 3.59 Å. As expected, the symmetry-related pseudo-octahedral Ni(II) centers in this complex have a Ni-N_{ArPy} distance (2.167(4) Å) that is longer than the Ni-N_{Py} distances (2.056(4) and 2.094(4) Å). The arrangement of the dimethoxyphenyl appendage results in a short aromatic C-H...arene arene centroid (pyridine) interaction (~3.7 Å) between the aryl-appended pyridyl and pyridyl donors on adjacent nickel centers.

This CH/π interaction is different than the others described herein in that the dimethoxyphenyl appendage of the chelate ligand acts as the C-H donor whereas in the other complexes methyl substituents of exogenous ligands coordinated to the metal center (e.g. methanol or acetonitrile) are the C-H donor in the CH/π interaction.[41]

Comparison of the structural features of the chloride complexes **19** and **22** provides evidence that increasing the number of aryl-appended pyridyl donors in the chelate ligand promotes the formation of a mononuclear cation in the solid state. Notably, conductivity studies indicate that **19** is a 1:1 electrolyte in acetonitrile,[36] whereas **22** behaves as a nonelectrolyte in dichloromethane.[28] This indicates that **19** retains its solid state structure in solution, whereas the outer sphere chloride anions in **22** must be coordinated in CH_2Cl_2, perhaps in a mononuclear [(6-(2,5-OMe_2Ph)TPA)$NiCl_2$] species. Complexes **18** and **20** are also 1:1 electrolytes in acetonitrile.[36]

The ^{1}H NMR features of **18–20** have been investigated in detail.[36] The paramagentically shifted resonances of these complexes were fully assigned using one- and two-dimensional ^{1}H NMR experiments and ^{2}H NMR of analogues having deuterium substitution in the phenyl appendages (using 6-(d_5-Ph)$_2$TPA) or methylene positions ((6-Ph)$_2$-d_6-TPA or (6-Ph)$_2$-d_2-TPA) of the supporting chelate ligand. Each complex has an α-H resonance in the region of 160–180 ppm and β/β′ resonances in the region of ~30–60 ppm. The γ/γ′ resonances are found in the range of 5–15 ppm and were assigned via observed coupling with the β/β′ resonances in ^{1}H–^{1}H COSY spectra. Thus, similar to aryl-appended Fe(II) complexes,[23] the pattern of isotropically shifted pyridine resonances (α-H > β-H > γ-H) is consistent with a σ-delocalization mechanism.

^{1}H NMR spectroscopic data has also been reported for **21**, albeit full assignment of the resonances was not completed.[31] For this complex, there are only two identifiable β-type signals at 68.0 and 46.3 ppm in CD_3CN. A resonance upfield of 0 ppm has been assigned as the amide N-H resonance as it disappears when D_2O is present in the CD_3CN solution. No ^{1}H NMR data has been reported for **22**.

The electrochemical properties of **18** were examined in acetonitrile under a N_2 atmosphere.[22] This complex exhibits a quasireversible Ni(II)/Ni(I) couple at −881 mV versus SCE measured at a scan rate of 100 mV/s.

The magnetic moment of **18** and **20**, measured using the Evans method,[50] is 3.2 μ_B for each complex. This is higher than the spin-only

value for Ni(II) (2.8 μ_B) due to spin-orbit coupling.[48] Similarly, **22** has a magnetic moment of 3.21 μ_B per Ni(II) center, as determined for a solid sample using a Guoy balance.[28]

Complexes **18–21** exhibit *d-d* transitions as expected for a pseudo-octahedral Ni(II) center. The binuclear chloride complex **22** exhibits three *d-d* absorption features at 420 ($\varepsilon = 180\,M^{-1}cm^{-1}$), 682 ($\varepsilon = 65\,M^{-1}cm^{-1}$), and 1170 nm ($\varepsilon = 68\,M^{-1}cm^{-1}$) when dissolved in dichloromethane.[28]

Cu(I). Two Cu(I) complex complexes of aryl-appended TPA ligands have been characterized by X-ray crystallography (Figure 12).[21,37] The binuclear Cu(I) complex of the 6-PhTPA ligand, $[((6\text{-Ph})TPACu)_2](PF_6)_2$ (**23**, Figure 12(a)) has one pyridyl arm of each chelate ligand bridging to the second copper center.[37] The solution ^1H NMR spectrum of **23** in d_6-acetone is consistent with the presence of a monomeric N_4-ligated Cu(I) species having mirror plane symmetry. Specifically, two benzylic proton resonances are found at 4.44 (2H) and 4.38 (4H) ppm, which is consistent with the presence of a plane of symmetry that includes the phenyl-appended pyridyl donor. $[(6\text{-}Ph_3TPA)Cu]BPh_4$ (**24**, Figure 12(b)) contains a distorted trigonal pyramidal Cu(I) center, which lies 0.32 Å above a plane containing the three pyridyl nitrogen donors.[21] The phenyl groups are arranged in a "T" configuration, which results in encapsulation of a fifth possible coordination site on the metal center. The ^1H NMR spectrum of **24** is consistent with three-fold symmetry in the cation when the complex is dissolved in $CDCl_3$.

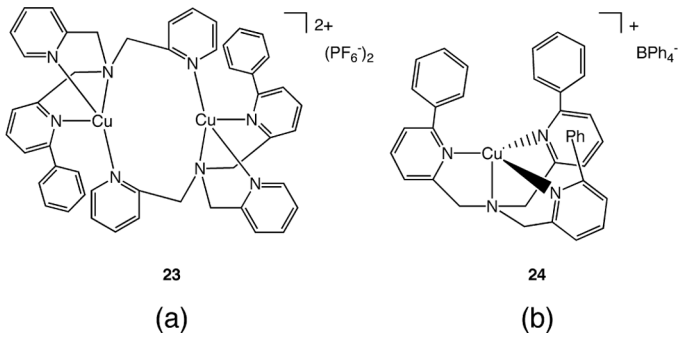

Figure 12. Drawings of the Cu(I) complexes **23** and **24**.

Cu(I) complexes of the 6-(2,5-$(OMe)_2$Ph)TPA and 6-(2,5-$(OH)_2$Ph)TPA ligands have been prepared and characterized by mass spectrometry, FTIR (solid-state) and ^{1}H NMR (in CD_3CN).[38] Results from the latter two methods are consistent with the aryl-appended pyridyl donor being non-coordinated in the solid state and solution.

Cu(II). Several mononuclear Cu(II) complexes of aryl-appended TPA ligands have been reported. The chloride complexes [(6-(2,5-$(OMe)_2$Ph)-TPA)Cu-Cl]PF_6[28] (**25**) and [(6-(2,5-OMe_2Ph)TPA)Cu-Cl]$Cl \cdot 3H_2O$[38] (**26,** (Figure 13(a)) have structurally similar cations, each containing a distorted square pyramidal Cu(II) center (**25**: $\tau = 0.15$; **26**: $\tau = 0.03$)[43] with one chloride ligand. For each, the aryl-appended pyridyl donor is in the axial position. Using a chelate ligand having hydroxyl appendages on the aryl group (6-(2,5-$(OH)_2$Ph)TPA), two mononuclear Cu(II) complexes have been isolated and characterized. The dichloride derivative [(6-(2,5-$(OH)_2$Ph)TPA)$CuCl_2$][38] (**27**, Figure 13(b)) exhibits κ^3-coordination of the chelate ligand, with the aryl-appended pyridyl donor not coordinated to the Cu(II) center. In this arrangement, the pyridyl nitrogen donor accepts a hydrogen bond from the hydroxyl substitutent of the aryl appendage. The geometry of the Cu(II) center in **27** is best described as slightly distorted square pyramidal ($\tau = 0.03$).[43] In [6-(2-O^--5-OHPh)TPA)Cu]PF_6 (**28**, Figure 13(c)) the Cu(II) center has a coordinated phenolate oxygen from the aryl appendage and a distorted trigonal bipyramidal geometry ($\tau = 0.71$).[38] In this cation, the deprotonated oxygen atom (Cu(1)-O(1) 1.899(4) Å) and the tertiary amine nitrogen atom (Cu(1)-N(4) 2.041(4) Å) are in the axial positions. Notably, whereas in **25** and **26** the shortest Cu-N distance (**25**: Cu-N(2) 1.984(3) Å; **26**: Cu-N(2) 1.991(6) Å) involves the nitrogen atom of an unsubstituted pyridyl donor, in **28** the shortest Cu-N bond (Cu-N(1) 1.978(4) Å) involves the aryl-appended pyridyl nitrogen atom.

Ligands having multiple aryl-appended pyridyl donors have been used to prepare two Cu(II) complexes, [((*rac*)-α-$MePh_2$TPA)-$Cu(NCCH_3)](ClO_4)_2$[39] (**29**) and [(6-Ph_3TPA)$Cu(NCCH_3)](ClO_4)_2$[21] (**30**). Drawings of these complexes are shown in Figure 13((d) and (e)), with **29** having a distorted trigonal bipyramidal Cu(II) center ($\tau = 0.66$)[43] and **30** exhibiting a trigonal bipyramidal geometry. In both **29** and **30** the Cu(II) ion sits $\geq$0.35 Å above the plane defined by the three pyridyl nitrogen donors.

The EPR and UV-visible spectroscopic properties of **25–28** have been reported.[28,38] For each complex, the spectral data is consistent

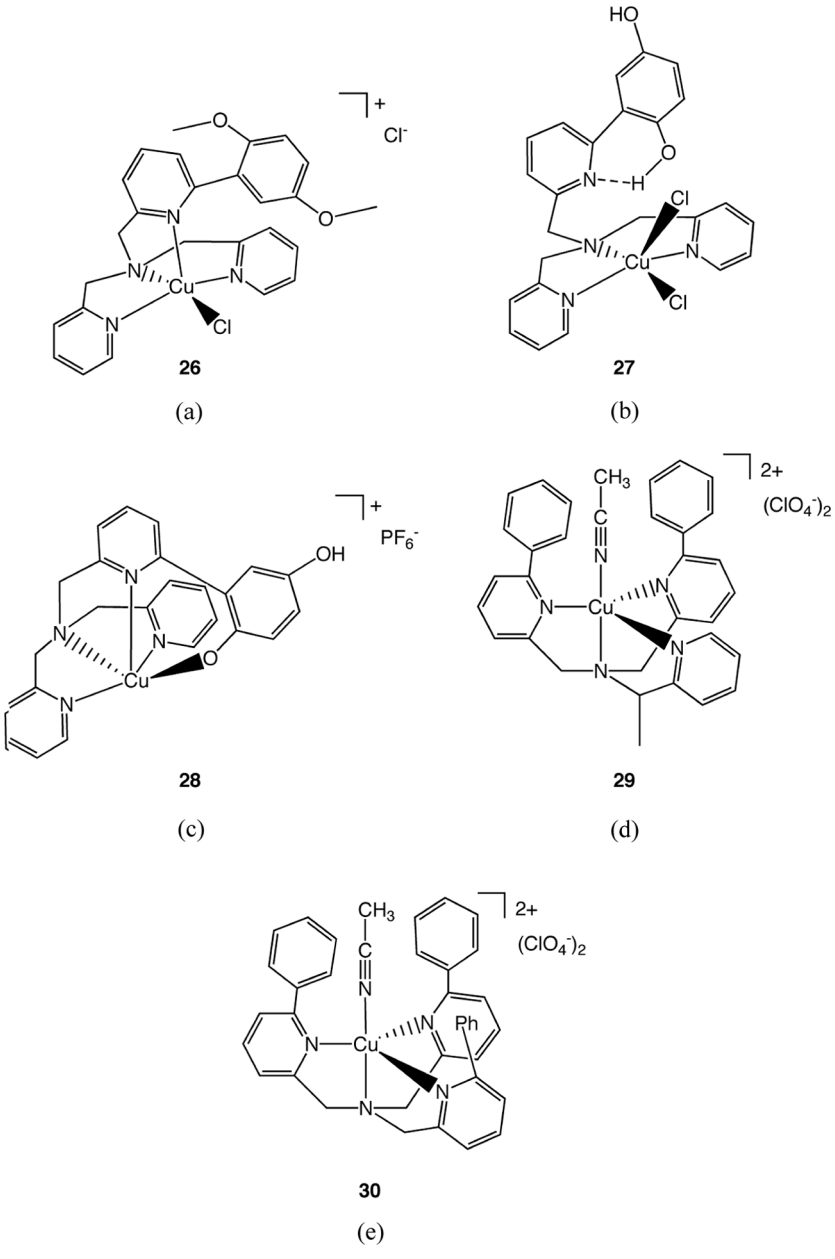

Figure 13. Drawings of the Cu(II) complexes **26**–**30**.

with retention of the observed solid-state copper coordination geometry in solution.

Cyclic voltammetry studies of **30** revealed that in various solvents the redox potential of this complex is positive (up to several hundred mV) relative to that of $[(TPA)Cu(NCCH_3)](ClO_4)_2$.[21,27] The more positive potential of **30** may be related to electron withdrawing effects of the phenyl substituents, or a reduction in the local dielectric due to steric shielding of the copper center by the phenyl groups. This shielding may limit access of a polar solvent to the metal center. A less polar environment would favor a lower charge on the metal center. The Cu(II) complexes $[(6\text{-}Ph_2TPA)Cu(NCCH_3)](ClO_4)_2$ and $[(6\text{-}PhTPA)Cu(NCCH_3)](ClO_4)_2$ were prepared to further examine how the hydrophobic phenyl appendages influence the electrochemical properties of the copper center in acetonitrile solution.[27] These studies revealed that each phenyl substituent imparts approximately a 100 mV increase in the redox potential of the metal center.

One additional Cu(II) complex, a tetranuclear copper carbonate derivative of the formulation $[\{(6\text{-}(2,5\text{-}(OMe)_2Ph)TPA)Cu\}_4(CO_3)_2](BF_4)_4 \cdot 5.2H_2O$ (**31**), has been produced upon treatment of the 6-(2,5-$(OMe)_2$Ph)TPA ligand with an equimolar amount of $[Cu(CH_3CN)_4]BF_4$, followed by bubbling of dioxygen into the reaction mixture.[28] The reaction sequence leading the formation of the carbonate complex was not examined in detail.

Zn(II). Five structurally characterized examples of mononuclear zinc complexes supported by aryl-appended TPA ligands have been reported to date.[22,28,31] The zinc chloride complex $[(6\text{-}(2,5\text{-}(OMe)_2Ph)\text{-}TPA)ZnCl_2]$ (**32**, Figure 14(a)) exhibits an overall coordination number of five, a distorted square pyramidal geometry ($\tau = 0.29$)[43] and a non-coordinated aryl-appended pyridyl appendage. One chloride anion is in an equatorial position (Zn-Cl(1) 2.234(1) Å) and the second is in the axial position (Zn-Cl(2) 2.244(1) Å).[28] ^{1}H NMR spectroscopic studies of **32** in $CDCl_3$ are consistent with retention of two coordinated pyridine donors and a non-coordinated aryl-appended pyridyl appendage in solution.[28]

The mononuclear zinc acetonitrile complexes of the 6-Ph_2TPA and 6-$(3,5\text{-}Me_2Ph)_2$TPA ligands, $[(6\text{-}Ph_2TPA)Zn(NCCH_3)](ClO_4)_2$ (**33**, Figure 14(b)) and $[(6\text{-}(3,5\text{-}Me_2Ph)_2TPA)Zn(NCCH_3)](ClO_4)_2$ (**34**, Figure 14(c)), each contain a distorted trigonal bipyramidal zinc center (**33**: $\tau = 0.79$; **34**: $\tau = 0.83$; 0.84 (two independent cations in the

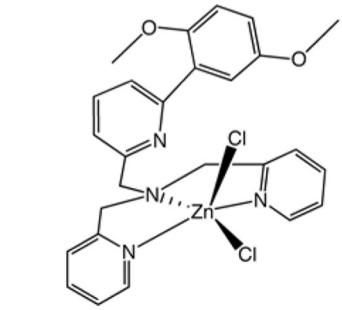

32

(a)

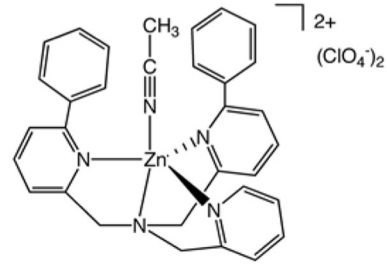

33

(b)

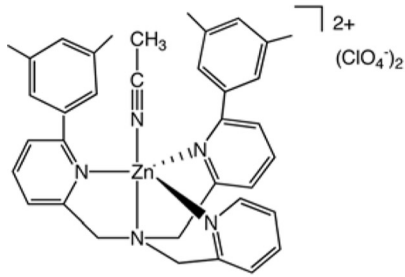

34

(c)

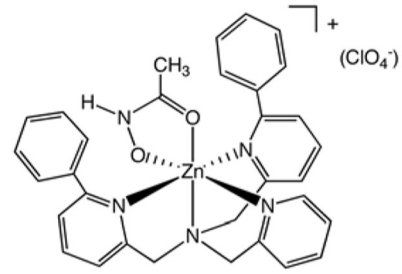

35

(d)

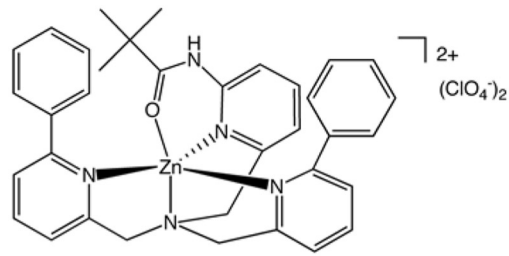

36

(e)

Figure 14. Drawings of the Zn(II) complexes **32–36**.

asymmetric unit)).[22,43] Both **33** and **34** contain weak CH/π interactions[41] between the methyl group of the coordinated acetonitrile ligand and the phenyl appendages of the chelate ligand.

The acetohydroxamate complex [(6-Ph_2TPA)Zn(ONHC(O)CH_3)]-ClO_4 (**35**, Figure 14(d)) has a distorted octahedral zinc center with the hydroxamate anion positioned between the phenyl appendages of the supporting chelate ligand.[22] Comparison of the structural features of **33** and **35** reveals that coordination of the bidentate anion results in significant elongation of the Zn-N_{PhPy} bond distances. In **33**, the Zn-N_{PhPy} distances are 2.139(2) and 2.075(2) Å whereas in **35** these distances are 2.679(2) Å and 2.219(2). The longer of these distances indicates only a weak interaction. The methyl group of the acetohydroxamate ligand forms a CH/π interaction[41] with a phenyl appendage of the ligand. Evidence for retention of this weak interaction in acetonitrile solutions of **35** comes from ^{1}H NMR wherein the acetohydroamate methyl resonance is found 0.34 ppm upfield (1.46 ppm) of its position in free acetohydroxamic acid (1.80 ppm).

The amide-appended bppppa ligand (Figure 1) coordinates to zinc to yield a distorted trigonal bipyramidal geometry in [(bppppa)Zn]-$(ClO_4)_2$ (**36**, Figure 14(e); $\tau = 0.63$). Unlike its Ni(II) analog, no interactions are found between the cation and the perchlorate anions in the solid state. A *tert*-butyl methyl group of the amide appendage forms weak CH/π interactions with the aryl appendages. These weak interactions are maintained in acetonitrile solutions of **36**, as evidenced by the upfield shift of the *tert*-butyl methyl ^{1}H NMR signal at 0.56 ppm relative to the chemical signal (1.24 ppm) of the same protons in the free ligand.

SUMMARY OF COORDINATION PROPERTIES

The coordination chemistry reported to date of aryl-appended tris(2-pyridylmethyl)amine ligands has revealed features imparted by this type of ligand that are common to many complexes. These include:

(1) M-N_{ArPy} distances that are longer than the M-N_{Py} distance(s) in the same complex. This is because the 6-aryl substitutent serves as both an electron-withdrawing group and as a steric hindrance with regard to the formation of the metal-ligand bond.

(2) Overall κ^3-coordination of the chelate ligand, with one non-coordinated aryl-appended pyridyl group, in the presence of coordinating anions (e.g. halides or triflate).
(3) A non-coordinated aryl-appended pyridyl group that can serve as an intramolecular hydrogen bond acceptor.
(4) More positive redox potentials for metal complexes with an increasing number of aryl appendages in the chleate ligand.
(5) Stabilization of metal-bound ligands through CH/π interactions.

These properties make aryl-appended tris(2-pyridylmethyl)amine ligands a useful alternative to the parent tris(2-pyridylmethyl)amine ligand for a variety of applications in synthetic bioinorganic chemistry (vida infra). In addition, the ease of deuterium substitution into the aryl appendages and benzylic positions of aryl-appended tris(2-pyridylmethyl)-amine ligands enables the extensive use of NMR (^{1}H and ^{2}H) for the characterization of paramagnetic complexes (e.g. Co(II) and Ni(II) derivatives) of these ligands.

BIOINORGANIC CHEMISTRY OF ARYL-APPENDED TRIS(2-PYRIDYLMETHYL)AMINE LIGANDS

Studies of the biologically-relevant chemistry of synthetic complexes supported by aryl-appended tris(2-pyridylmethyl)amine ligands have only recently begun to appear in the literature. Importantly, the aryl appendages have been shown to serve as a substrate in iron-mediated aromatic hydroxylation reactions[23,35] and as a hydrophobic microenvironment in Ni(II) complexes of relevance to acireductone dioxygenases.[51–53] Notably, while both of these systems involve reactions with dioxygen, the former involves the formation and reactivity of a high valent iron (IV) oxo species, whereas the latter involves dioxygen reactivity with a Ni(II)-coordinated substrate. Other biologically relevant applications of aryl-appended tris(2-pyridylmethyl)amine ligands include the development the first reactive model system for Ni(II)-containing glyoxalase I[54] and the isolation of a novel Ni(II) acetohydroxamic acid of relevance to a proposed weak enzyme/inhibitor complex in urease enzymes.[30,31]

Iron-promoted Aromatic Hydroxylation Reactivity. Phenyalanine (PheH), tyrosine (TyrH) and tryptophan (TrpH) hydroxylase are non-heme iron(II)- and pterin-dependent enzymes that catalyze the hydroxylation of an aryl amino acid.[55–63] In the catalytic cycle of these enzymes

an Fe(IV)=O moiety has been proposed to act as an electrophile toward the aromatic substrate.[55,63,64] In a model study of functional relevance to these enzymes, it was found that treatment of an acetonitrile solution of **4** (Figure 3(a)) with ^{t}BuOOH (3 eq) under an argon atmosphere results in the oxidative hydroxylation of the ligand phenyl ring (Scheme 2).[23,35] To isolate the final product of this reaction, base (NEt_3) and $NaBPh_4$ were added in wet methanol, which resulted in the deposition of $[(6\text{-}C_6H_4O\text{-}TPAFe)_2(\mu\text{-}O)](BPh_4)_2$ (**37**). In the absence of NEt_3 and $NaBPh_4$, a mixture of the cations $\{[(6\text{-}C_6H_4O\text{-}TPAFe)_2(\mu\text{-}O)](ClO_4)\}^+$ and $[(6\text{-}C_6H_4O\text{-}TPA)Fe(ClO_4)]^+$ was detected by mass spectrometry.[23] Complex **37** was characterized by multiple methods, including X-ray crystallography. In the binuclear cation the symmetry related Fe(III) centers each exhibit coordination of a phenolate oxygen atom as well as all of the nitrogen donors of the chelate ligand. A bridging oxo group completes the coordination environment of each Fe(III) center.

For the reaction outlined in Scheme 2, at low temperature (-60°C) a transient intermediate was identified using UV-vis, resonance Raman, and EPR spectroscopy. This intermediate, which is formulated as an Fe(III) alkylperoxide species $[(6\text{-PhTPA})Fe^{III}(OO\mathit{t}Bu)]^{2+}$ (**38**, Scheme 3),[35] decays over a period of $\sim$4 hours at -60°C to give a second intermediate prior to the formation of **37**. Isotope labeling studies provided evidence that the oxygen atom that is incorporated into the ligand aryl appendage is derived from the terminal peroxide oxygen atom. These studies also indicated that the active oxidant in this system can undergo exchange with the oxygen atom of water. Based on this and additional evidence, the reactive species for aromatic hydroxylation was formulated

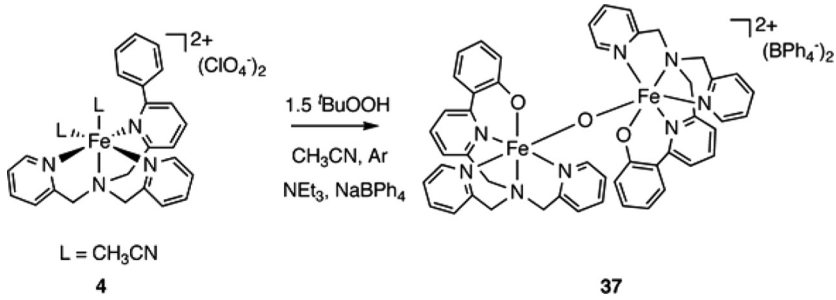

Scheme 2. Aromatic hydroxylation reaction of **4** upon treatment with ^{t}BuOOH.

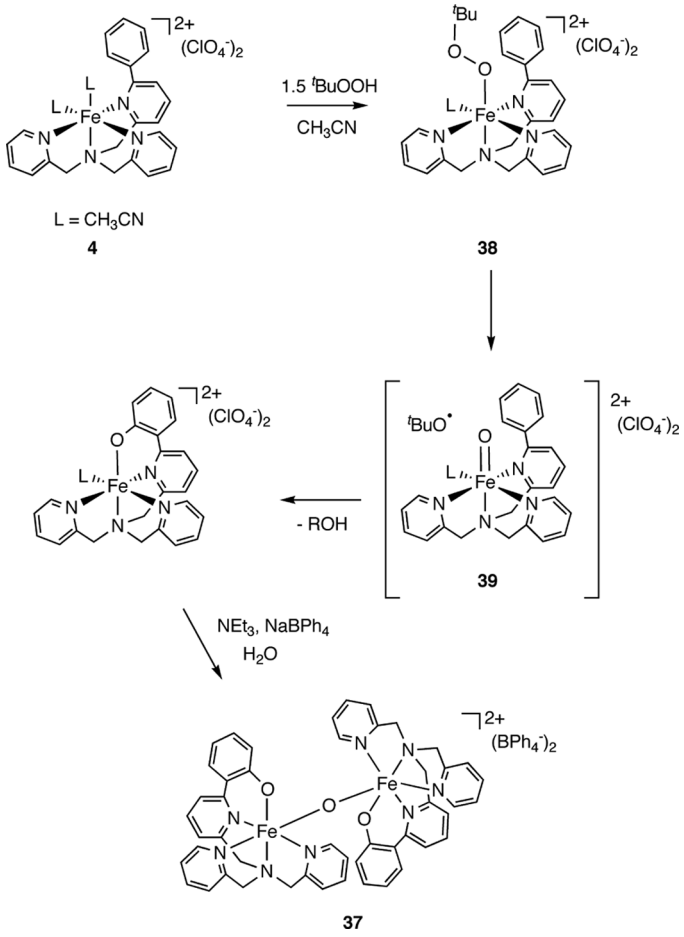

Scheme 3. Proposed reaction pathway for the formation of **37** upon treatment of **4** with ^{t}BuOOH.

as $[(6\text{-PhTPA})Fe^{IV}{=}O]^{2+}$ (**39**, Scheme 3).[23] Notably, use of the d_1-6-PhTPA ligand, wherein a deuterium atom is incorporated at one of the two *ortho* positions of the aryl group, results in no selectivity in terms of the site of arene hydroxylation, but a significant amount of "NIH-shift" (1,2-deuterium shift) product was identified. This is consistent with the reactivity of an electrophilic oxidant such as $[(6\text{-PhTPA})Fe^{IV}{=}O]^{2+}$. A proposed mechanism for the reaction of **4** with ^{t}BuOOH to generate **37** is shown in Scheme 3. It is worth noting that

treatment of **4** with iodosobenzene also results in aromatic ring hydroxylation.[65]

Iron-promoted Aromatic Amination Reactivity. Similar to the arene hydroxylation reactivity exhibited by **4** in the presence of iodosobenzene (PhIO), treatment of **4** with phenyl-*N*-tosylimidoiodinane (Scheme 4) yields $[(6\text{-}C_6H_4NTs\text{-}TPA)Fe(CH_3CN)]^{2+}$ (**40**) in a novel example of an aromatic amination reaction.[65] The reaction pathway for the formation of **40** is suggested to involve a reactive Fe(IV)=NTs intermediate.

Copper-Dioxygen Chemistry. Aromatic hydroxylation reactions promoted by copper complexes are of relevance to the active site chemistry of tyrosinase.[66] In this regard, multiple laboratories have reported arene hydroxylation reactions involving reactive complexes having a (μ-η^2:η^2-peroxo)dicopper(II) or bis(μ-oxo)dicopper(III) core.[67–76] Based on the observed arene hydroxylation reactivity of the Fe(II) compound of 6-PhTPA (**4**),[23,35] and arene hydroxylation reactivity in a previously reported Cu/O_2 system of a bidentate ligand containing an aryl-appended pyridyl donor,[76] Que and coworkers investigated the dioxygen reactivity of $[(6\text{-PhTPA})Cu]SbF_6$ (an analog of **23**, Figure 12(a)). At low temperature, this reaction results in the formation of a thermally unstable dicopper(III) bis(μ-oxo) complex $[(6\text{-PhTPACu}^{III})_2(\mu\text{-}O)_2](SbF_6)_2$ (**41**).[37] The spectroscopic signatures of this complex include $\lambda_{max} = 378$ nm and an ^{18}O-sensitive vibration in the resonance Raman spectrum at 599 cm^{-1}. Decomposition of **41** yields Cu(II) complexes of the intact 6-PhTPA ligand. Notably, these Cu(II) products show no evidence for the hydroxylation of the phenyl appendage of the 6-PhTPA ligand, or *N*-dealkylation chemistry. The absence of arene hydroxylation chemistry is likely due to the phenyl-appended pyridyl moiety being in the axial position of a square pyramidal Cu(II) center.

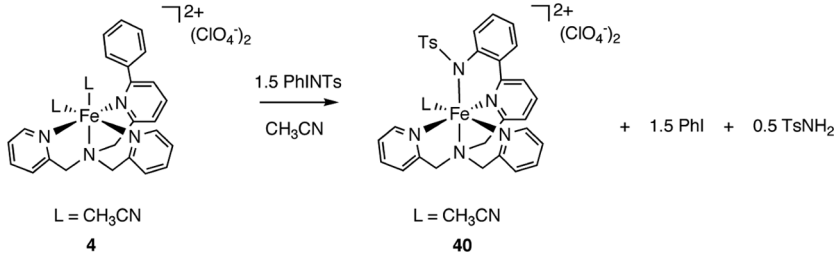

Scheme 4. Aromatic amination reaction of **4** upon treatment with PhINTs.

A Model Complex for Ni(II)-Containing Acireductone Dioxygenase. Acireductone dioxygenases (ARDs) are metalloenzymes associated with the methionine salvage pathway in species ranging from bacteria to mammals.[77–81] Two ARD enzymes having the same protein component, but which differ in the nature of the active site metal ion present (Fe(II) or Ni(II)) have been identified in *Klebsiella pneumoniae*.[80] Interestingly, these enzymes catalyze the O_2-dependent oxidation of 1,2-dihydroxy-3-oxo-(S)-methylthiopentene (an acireductone, Scheme 5) to give different products. Specifically, the Fe(II)-containing enzyme catalyzes a reaction that yields a precursor to methionine whereas the Ni(II) enzyme catalyzes a reaction that is a shunt out of the methionine salvage pathway and results in the formation of a methylthiocarboxylic acid, formic acid, and carbon monoxide.

Recently, X-ray absorption and NMR spectroscopic studies have provided insight into the ligand environment of the metal centers in these M(II)-ARD enzymes.[82–86] For both enzymes, the resting state metal center is ligated by three histidine residues, one carboxylate, and two water molecules. Introduction of the acireductone substrate under anaerobic conditions results in the displacement of the metal-bound water molecules and formation of an enzyme/substrate adduct wherein the substrate coordinates to the metal center as either a

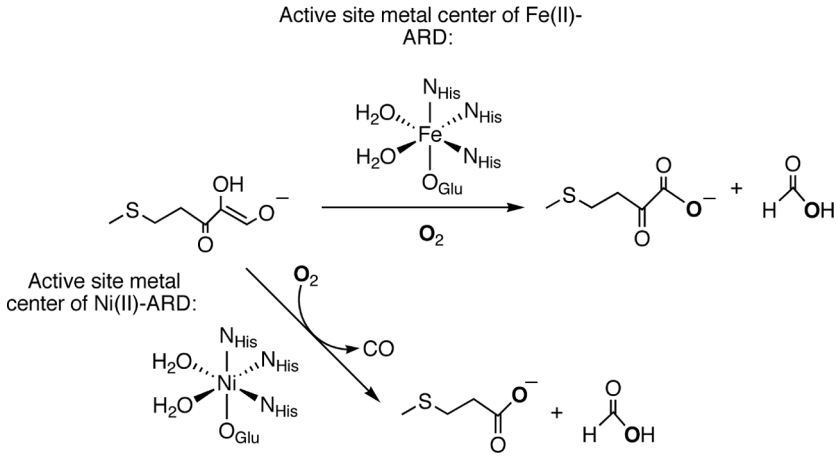

Scheme 5. Reactions catalyzed by acireductone dioxygenases. Reprinted with permission from reference 52. © 2007 American Chemical Society.

five- or six-membered chelate ring.[85] The smaller chelate ring is suggested to correlate with the formation of Fe(II)-ARD type products (α-ketoacid and formate) upon reaction with dioxygen, whereas the larger chelate ring is suggested for the O_2-dependent reaction catalyzed by the Ni(II)-ARD enzyme. A proposed mechanism for the Ni(II)-ARD catalyzed reaction has been put forth (Scheme 6).[82,83]

To gain insight into the chemistry of species of relevance to the enzyme/substrate adduct in Ni(II)-ARD, we initiated studies of the coordination chemistry of the bulky acireductone model substrate 2-hydroxy-1,3-diphenylpropan-1,3-dione (Figure 15).[51,52] While not an exact replica of the acireductone substrate, use of this bulky derivative has enabled the isolation of a novel Ni(II) complex that is reactive with O_2.[51,52]

As shown in Scheme 7, working under a N_2 atmosphere, treatment of 6-Ph_2TPA with equimolar amounts of $Ni(ClO_4)_2 \cdot 5H_2O$, $Me_4NOH \cdot 6H_2O$, and the bulky model substrate yields [(6-Ph_2TPA)-Ni(PhC(O)C(OH)C(O)Ph)]ClO_4 (**42**).[51] In this complex, the bulky acireductone model substrate is coordinated as a monoanion in a bidentate fashion. It is positioned between the two phenyl appendages in a motif that may be relevant to the active site chemistry of Ni(II)-ARD.

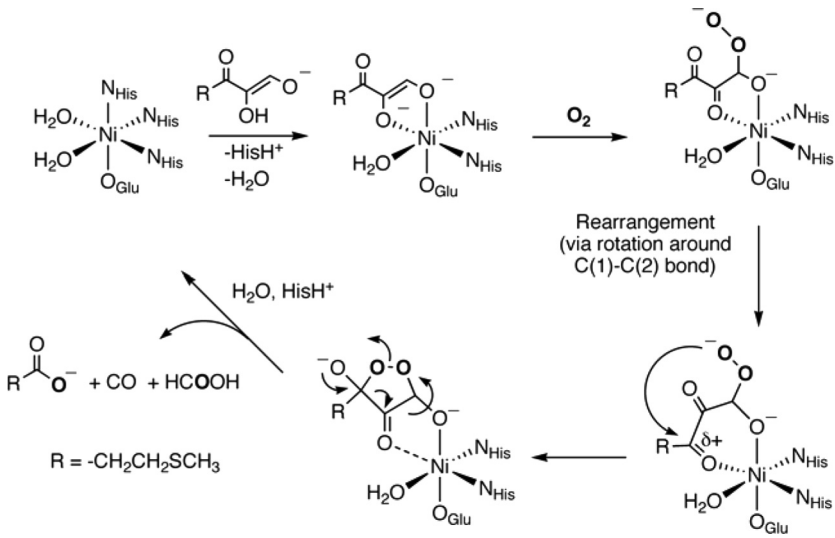

Scheme 6. Proposed mechanism for acireductone oxidation catalyzed by Ni(II)-ARD. Reprinted with permission from reference 52. © 2007 American Chemical Society.

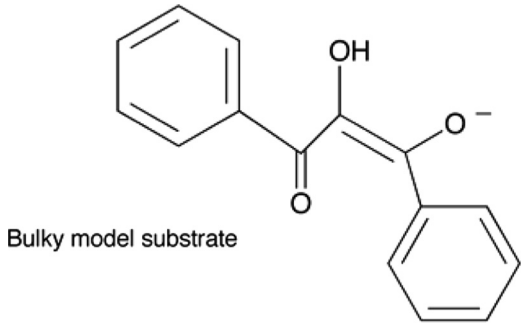

Figure 15. Bulky acireductone model substrate.

Specifically, the side chains of two phenylalanine residues in the Ni(II)-ARD active site are located close enough to the metal center to exhibit paramagentically shifted ^{1}H NMR resonances and are proposed to help orient the substrate.[83] In **42**, the phenyl appendages form a "sandwich"-type motif with the coordinated model substrate.

When dissolved in acetonitrile **42** yields an orange-brown solution with an absorption maximum at 399 nm.[51,52] This absorption feature shifts to 420 nm upon addition of one equivalent of $Me_4NOH \cdot 5H_2O$. This suggests that the coordinated bulky model substrate undergoes deprotonation. Addition of O_2 to the 420 nm species results in an immediate bleaching of the orange-brown color and formation of a Ni(II) complex having two coordinated benzoate ligands (**43**, Scheme 8). In the absence of added base, **42** undergoes reaction with O_2 to yield the monobenzoate complex **44**. In both of these reactions CO is produced, as well as small amounts of organic byproducts

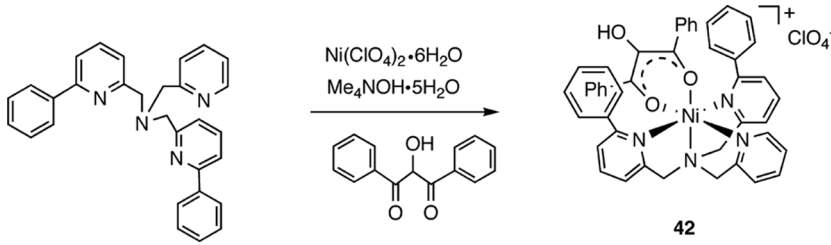

Scheme 7. Synthetic route for the preparation of **42**. Reprinted with permission from reference 51. © 2005 American Chemical Society.

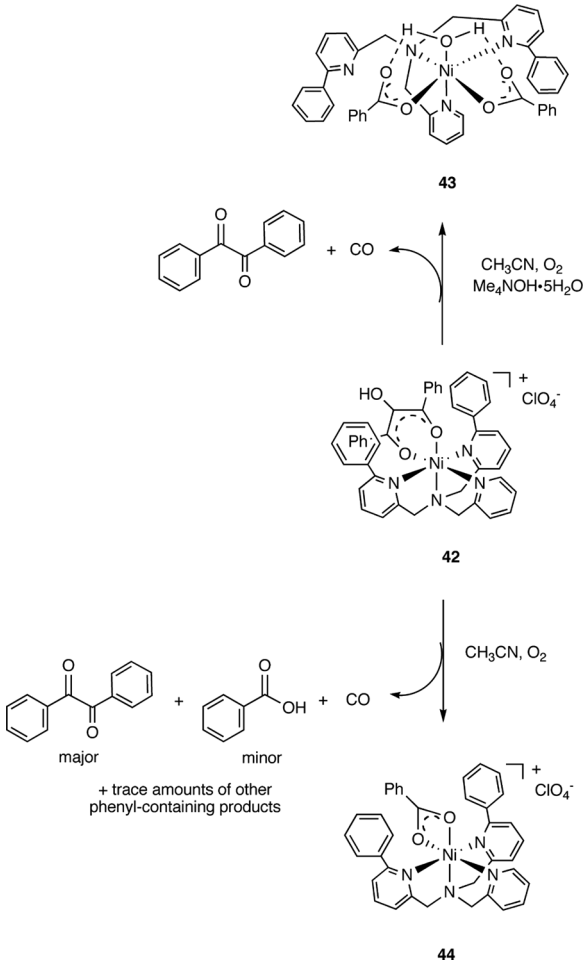

Scheme 8. Reaction of **42** with O_2 in the presence and absence of base. Reprinted with permission from reference 53. © 2007 American Chemical Society.

(e.g. benzil). Overall, the reaction wherein the proposed dianionic form of the bulky model substrate has been generated is cleaner, with only one organic byproduct (benzil) and a higher level of ^{18}O incorporation in the carboxylate ligands of **43** (~67%) versus that found in **44** (~50%).[51,52] These are the first reported model reactions for Ni(II)-ARD. Additional kinetic and mechanistic studies of these reactions are currently in progress.

The carboxylate complex **43** can be converted to the monobenzoate derivative **44** upon treatment with ammonium perchlorate (Scheme 9).[53] Notably, **44** undergoes a carboxylate shift from bidentate to monodentate in the presence of water, yielding the six-coordinate **45** (Scheme 9).

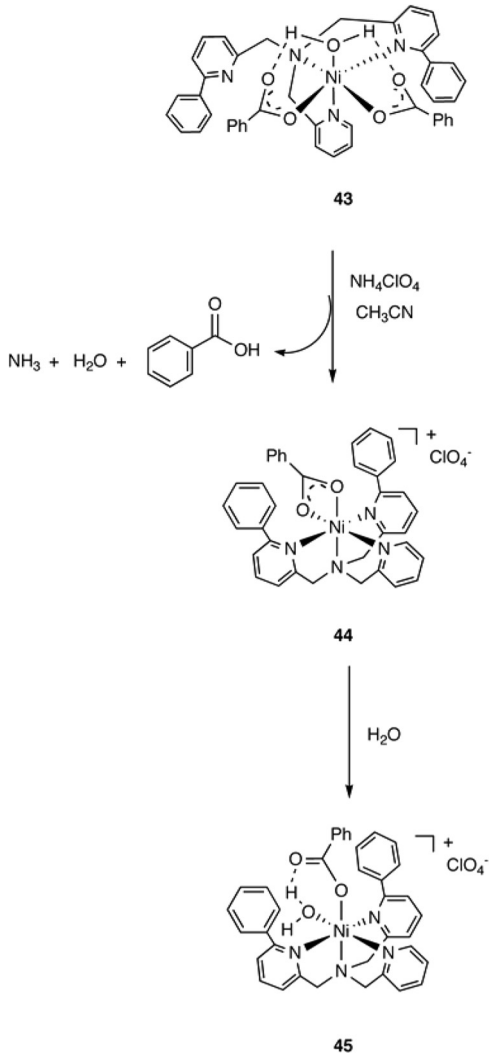

Scheme 9. Reactivity of Ni(II) carboxylate complexes. Reprinted with permission from reference 53. © 2007 American Chemical Society.

Similar reactivity is found for Ni(II) methylthiopropionate and methylthioacetate complexes of the 6-Ph_2TPA ligand. However, water-dependent carboxylate shift chemistry is not found for Ni(II) monocarboxylate complexes of the *N*,*N*-bis((6-neopentylamino-2-pyridyl)methyl)-*N*-((2-pyridyl)methyl)amine (bnpapa) ligand, which contains secondary hydrogen bond donor amine appendages instead of the phenyl appendages found in 6-Ph_2TPA. These results provide evidence that the nature of the secondary environment in the active site of Ni(II)-ARD may influence the chemistry of Ni(II)-carboxylate species produced following substrate oxidation.

Neutral Acetohydroxamic Acid Coordination to a Mononuclear Ni(II) Center. Relevance to the Chemistry of Urease. Acetohydroxamate anion is a well-known inhibitor of metalloenzymes, including ureases.[87–91] These enzymes, which contain a binuclear Ni(II) site, initially form a weak enzyme/inhibitor complex between acetohydroxamic acid (*E*-1, Scheme 10) and one of the two Ni(II) centers.[92–94] From the *E*-1 species, a more stable bridging acetohydroxamate species (*E*-1*) forms. Although binuclear Ni(II) complexes relevant to the *E*-1* species have been previously reported,[95,96] prior to 2005, no report of a neutral acetohydroxamic acid complex of relevance to the *E*-1 species had appeared in the literature.

We found that treatment of [(bppppa)Ni]$(ClO_4)_2$ (**21**, Figure 10(d)) with an equivalent of acetohydroxamic acid results in the formation of [(bppppa)Ni(HONHC(O)CH_3)]$(ClO_4)_2$ (**46**, Scheme 11),[30,31] a novel mononuclear Ni(II) acetohydroxamic acid complex with some relevance to the proposed weak enzyme/inhibitor complex of urease (*E*-1, Scheme 10).[92–94] In **46**, the acetohydroxamic acid coordination is stabilized by a hydrogen bonding interaction between the hydroxyl proton of

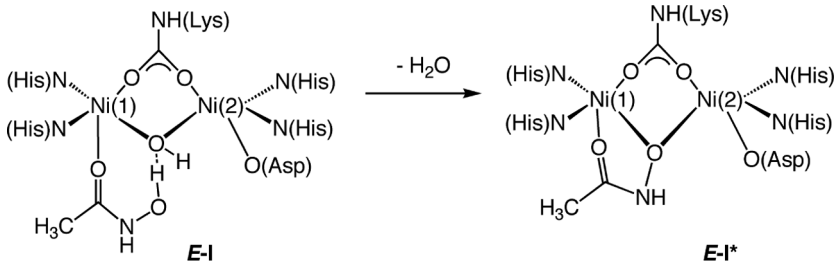

Scheme 10. Inhibition of urease with acetohydroxamate anion [30]. Reproduced with permission of The Royal Society of Chemistry.

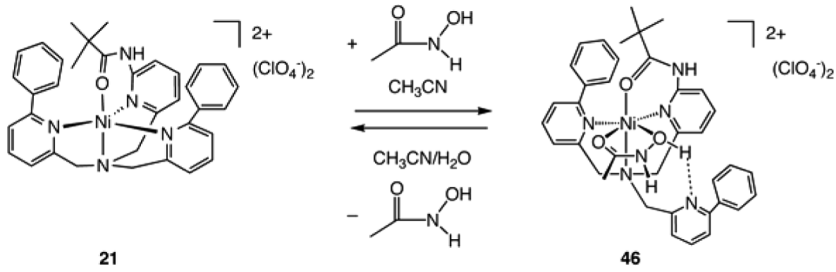

Scheme 11. Acetohydroxamic acid coordination chemistry involving a mononuclear Ni(II) complex. Reprinted with permission from reference 21. © 2006 American Chemical Society.

the Ni(II)-coordinated acid and the non-coordinated aryl-appended pyridyl moiety. Notably, treatment of **46** with excess water results in the formation of **21** and free acetohydroxamic acid. This release of the acid likely occurs due to the break-up of the hydrogen-bonding interaction in the presence of water.

A Reactive Model Complex for Ni(II)-Containing Glyoxalase I. The glyoxalase pathway involves two enzymes (glyoxalase I and glyoxalase II) and is responsible for the detoxification of cytotoxic 2-oxoaldehydes (e.g. methyl glyoxal, $CH_3C(O)C(O)H$).[97] As outlined in Scheme 12, glyoxalase I catalyzes the isomerization of a hemithioacetal to produce a thioester. Glyoxalase II catalyzes the hydrolysis of this thioester to produce free glutathione and a carboxylic acid. Several glyoxalase I enzymes have been found to contain Ni(II) as the active site metal ion.[98–100] An X-ray structure of the glyoxalase I enzyme from *E. coli* revealed that the Ni(II) center is ligated by a mixture of nitrogen and oxygen donor ligands, $[(NHis)_2(OGlu)_2Ni(OH_2)_2]$.[101] A mechanistic pathway for the reaction catalyzed by *E. coli* glyoxalase I has been put forth on the basis of X-ray absorption spectroscopic studies (Scheme 13). In this pathway, a Ni-OH is proposed to deprotonate the hemithioacetal, followed by transfer of a proton from a Ni-OH_2 moeity to the former carbonyl carbon in the enolate anion. It is unclear whether the intermediate enenolate anion interacts with the active site Ni(II) center during the catalytic cycle.

To date, a synthetic Ni-OH complex has not been shown to promote the isomerization of a hemithioacetal. In an attempt to prepare a mononuclear Ni-OH complex for subsequent hemithioacetal isomerization

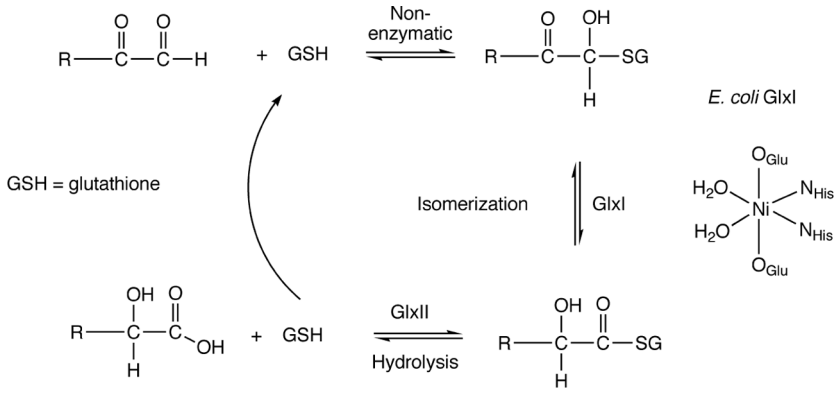

Scheme 12. Glyoxalase pathway. Reprinted with permission from reference 54. © 2006 American Chemical Society.

reactivity studies, we treated [(bppppa)Ni]$(ClO_4)_2$ (**21**, Figure 10(d)) with one equivalent of $Me_4NOH \cdot 5H_2O$ in acetonitrile.[54] Interestingly, this reaction did not result in the formation of a Ni-OH complex, but instead a deprotonated amide complex, [(bppppa$^-$)Ni]ClO_4 (**47**, Figure 16), was isolated. This complex was characterized by X-ray crystallography, ^{1}H NMR, FTIR, UV-vis, and elemental analysis. The Ni(II) center exhibits a geometry that is intermediate between square pyramidal and trigonal bipyramidal.

Although **47** does not contain a Ni-OH moiety, it does contain a coordinated anion in the form of the deprotonated amide. Interestingly, we found that treatment of **47** with the deuterium-labeled hemithioacetal $PhC(O)CH(OH)SCD_3$ in dry acetonitrile at 302 K results in hemithioacetal isomerization in $\sim$60% yield after $\sim$1.5 h (Scheme 14), with the thioester product being detected by ^{2}H NMR. A control reaction involving the parent complex **21** (Figure 10(d)) indicated that the deprotonated amide moiety in **47** is required for hemithioacetal isomerization reactivity. Studies involving treatment of a simple Ni(II) salt ($NiBr_2 \cdot 2H_2O$) with $PhC(O)CH(OH)SCD_3$ in the presence of 1-methylpyrrolidine revealed a reaction that, while also yielding some thioester product, is slower and involves the formation of multiple $-SCD_3$ labeled species, as detected by ^{2}H NMR. Overall, these combined results provided initial evidence that the well-defined coordination complex **47**, which has a basic ligand component, will promote cleaner hemithioacetal isomerization reactivity than a simple Ni(II) ion in the presence of base.

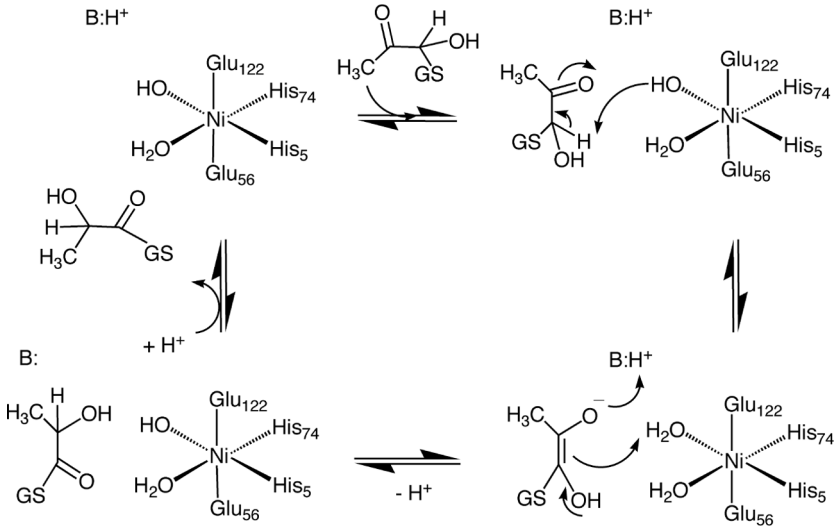

Scheme 13. Proposed reaction pathway for glyoxalase I involving a Ni-OH species. Reprinted with permission from reference 54. © 2006 American Chemical Society.

COMMENTS ON THE USE OF ARYL-APPENDED TPA LIGANDS

The Canary laboratory reported the first synthesis and use of aryl-appended TPA ligands in 1995.[21,27] They were interested in using such ligands to develop complexes for molecular recognition studies and to investigate how a hydrophobic microenvironment influences the redox

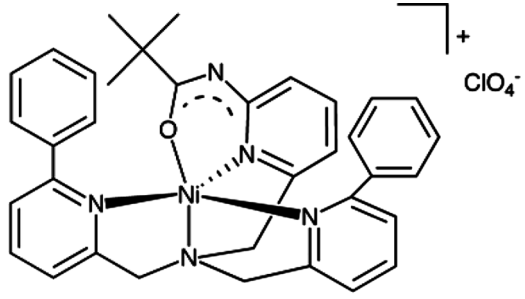

47

Figure 16. Drawing of the deprotonated amide Ni(II) complex **47**.

potential of biologically relevant copper complexes. An interesting finding in regard to the second area was the discovery that the 6-Ph_3TPA ligand stabilizes the Cu(I) oxidation state and that [(6-Ph_3TPA)Cu]PF_6 is unreactive with O_2. This lack of reactivity may be due to the positive redox potential of the complex, although steric constraints may also limit O_2 access and/or coordination to the copper center.

The next chemistry to be reported involving an aryl-appended TPA ligand was the identification by Larry Que and coworkers of arene hydroxylation reactivity upon treatment of [(6-PhTPA)Fe$(CH_3CN)_2$]$(ClO_4)_2$ (**4**) with ^{t}BuOOH (Scheme 2). This work, as well as follow-up studies from the same laboratory, is significant for a number of reasons. First, the observed arene hydroxylation chemistry demonstrated that the phenyl appendage of the 6-PhTPA ligand was appropriately positioned to be a model substrate for reactions involving an iron-centered oxidant. Mechanistic studies revealed the active oxidant for arene hydroxylation to be an Fe(IV)=O species (Scheme 3). Que and coworkers took advantage of the "proximity" of the phenyl appendage to also examine aromatic amination reactivity in the reaction of **4** with PhI=NTs (Scheme 4).[65] Mechanistic studies of this novel reaction suggest the involvement of an Fe(IV)=NTs species. These preliminary studies have opened up a new area of investigation involving comparing the chemical properties and reactivity of Fe(IV)=O versus Fe(IV)=NR species.[65,102]

Notably, the reaction of [(6-PhTPA)Cu]SbF_6 with O_2 does not result in arene hydroxylation.[37] In this case, a dicopper(III) bis(μ-oxo) complex is formed wherein the phenyl-appended pyridyl moiety is apparently not positioned correctly to undergo arene hydroxylation, as dicopper(III) bis(μ-oxo) species have been previously shown to undergo this type of reaction.[76] To date, well defined dioxygen reactivity has not been reported for any other metal complex of an aryl-appended TPA ligand.

Since 2001, the research laboratory of Dominique Mandon has reported several studies of the Fe(II) and Fe(III) coordination chemistry of various aryl-appended TPA ligands.[20,24,25,34] This work has yielded important insight into how halide ligands affect the coordination properties of aryl-appended TPA ligands. Studies from the laboratory of Stephen Colbran reported in 2002 and 2003 provided insight into the coordination chemistry of mono aryl-appended TPA ligands with a variety of metal halides.[28,38]

We began our studies of the coordination chemistry of the 6-Ph_2TPA ligand with an interest in using this ligand to construct model complexes

for enzymes of the cupin superfamily.[103–105] Members of this family include acireductone dioxygenases and oxalate decarboxylase. Metalloenzymes of this family have in common an active site metal center ligated by three histidine ligands, one glutamate, and two *cis* water molecules (see acireductone active site drawing, Scheme 5). Mechanistic pathways have been proposed for these enzymes wherein the substrate (acireductone or oxalate) coordinates to the metal center prior to reaction with O_2.[86,106] Our decision to initially use 6-Ph_2TPA in our chemistry was based on the identification of two phenylalanine residues in the active site of Ni(II)-ARD that were close enough to the Ni(II) center to exhibit paramagnetically shifted resonances.[83]

Based on the halide ligand effects demonstrated in the work of Mandon and Colbran, our initial work focused on the preparation and characterization of synthetic divalent metal complexes, including Ni(II) and Mn(II) derivatives, having non-coordinating anions. We hypothesized that such complexes could serve as precursors for the construction of substrate-adduct type complexes. Interestingly, we found that while the 6-Ph_2TPA ligand coordinated in a tetradentate fashion to Ni(II) in [(6-Ph_2TPA)-Ni(CH_3CN)(CH_3OH)](ClO_4)$_2$ (**18**, Figure 10), tridentate coordination of the chlelate ligand was found in the Mn(II) complex ([(6-Ph_2TPA)Mn(CH_3OH)$_3$]-(ClO_4)$_2$ (**2**, Figure 2)). Generation of hydroxamate complexes for both metal ions also revealed different coordination properties for the chelate ligand, with the Ni(II) complex being mononuclear [(6-Ph_2TPA)-Ni(ONHC(O)CH_3)]ClO_4 (**20**, Figure 10) and the Mn(II) hydroxamate complex, [(6-Ph_2TPAMn)$_2$(μ-ONHC(O)CH_3)$_2$](ClO_4)$_2$ (**3**, Figure 2), being binuclear with bridging hydroxamate anions and κ^3-coordination of the 6-Ph_2TPA ligand at each Mn(II) center.

In terms of developing reactive synthetic model systems for acireductone dioxygenases, we recently demonstrated that a 6-Ph_2TPA-ligated Ni(II) complex having a bulky acireductone model substrate can be prepared and characterized.[51] In the presence of an equivalent of base, this complex (**42**, Scheme 8) undergoes reaction with dioxygen to give ARD-type products, CO and carboxylates, the latter of which remain coordinated to the Ni(II) center. Importantly, we discovered that the protonation level of the coordinated substrate (dianionic vs. monoanionic) influences the nature of the products generated in the reaction.[52] Using this system, we are now uniquely positioned to examine in detail the mechanism of the acireductone oxidation reaction, and the influence of coordination environment (both primary and secondary)

on the oxidation reaction. Current efforts are also focused on extending these studies to examine the Ni(II) and Fe(II) coordination chemistry of acireductone analogs having a C(1)-H moiety, versus the bulky model substrate (Figure 15), which has a C(1)-Ph group. These sterically smaller acireductones are alternative substrates for ARD enzymes.[107]

As noted above, tridentate coordination of the 6-Ph_2TPA ligand is found in the Mn(II) complexes **2** and **3** (Figure 2). This type of coordination for the 6-Ph_2TPA ligand is also found in a binuclear Mn(II) oxalate complex, [(6-Ph_2TPAMn(CH_3OH))$_2$(μ-C_2O_4)](ClO_4)$_2$ (**48**).[108] The oxalate dianion in **48** is coordinated in a bis-bidentate fashion, as has been identified in other binuclear Mn(II) oxalate complexes.[109,110] Similar to [(6-Ph_2TPA)Mn(CH_3OH)$_3$](ClO_4)$_2$ (**2**) the Mn(II)-coordinated methanol molecule in **48** participates in a hydrogen bonding interaction with the non-coordinated phenyl-appended pyridyl moiety.

Our combined results to date in terms of using the 6-Ph_2TPA ligand to produce model complexes for metalloenzymes of the cupin superfamily indicate that while mononuclear Ni(II) complexes relevant to acireductone dioxygenases can be isolated, characterized, and their reactions with O_2 evaluated, multinuclear chemistry dominates for Mn(II) complexes. Therefore, while our work with 6-Ph_2TPA continues for modeling the chemistry of ARD enzymes, other ligand structures are being explored in attempts to stabilize a mononuclear Mn(II) oxalate complex.

A new type of chelate ligand that we began investigating for modeling metalloenzymes of the cupin superfamily is an analog of 6-Ph_2TPA (bppppa, Figure 1) that contains a hydrogen bond donor amide moiety incorporated at the *ortho* position of the formerly unsubstituted pyridyl donor. During initial attempts to prepare a Ni(II) hydroxamate complex of this ligand, we found that the bppppa-ligated Ni(II) center forms a complex with neutral acetohydroxamic acid, [(bppppa)Ni(HONHC(O)CH_3)](ClO_4)$_2$ (**46**, Scheme 11) wherein the acid coordination is stabilized by a hydrogen bonding interaction involving a non-coordinated phenyl-appended pyridyl moiety. The coordinated acid in this complex can be displaced upon treatment with water. These combined results have relevance to a proposed acetohydroxamic acid adduct in the active site of urease (Scheme 10). In our opinion, the isolation of **46** could not have been predicted on the basis of literature precedent, as this is the first example of neutral acetohydroxamic acid coordination to any metal center. Such a discovery argues for the continued study of the coordination chemistry of aryl-appended TPA ligands.

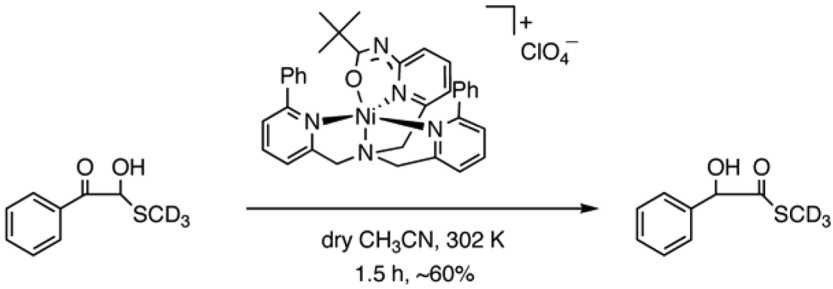

Scheme 14. Reaction of **47** with a deuterium-labeled hemithioacetal. Reprinted with permission from reference 54. © 2006 American Chemical Society.

Our discovery of hemithioacetal isomerization reactivity for the deprotonated amide complex **47** (Scheme 14) revealed a novel example of intermolecular acid/base reactivity involving a metal-coordinated amide moiety. Again, this biologically relevant reactivity would not have been predicted on the basis of previously reported coordination chemistry of amides. Current efforts in our laboratory are focused on investigating the scope of this reactivity as a function of the metal ion and chelate ligand structure.

As outlined herein, over the past ~12 years aryl-appended TPA ligands have been used to produce a wealth of new compounds. We look forward to more exciting discoveries as we continue to investigate the coordination and bioinorganic chemistry of these ligands.

ACKNOWLEDGMENTS

Financial support from the National Institutes of Health, the National Science Foundation, and the Herman Frasch Foundation is gratefully acknowledged.

REFERENCES

1. Blackman, A. G. 2005. The coordination chemistry of tripodal tetraamine ligands. *Polyhedron*, **24**, 1–39.
2. Berreau, L. M. 2006. Bioinorganic chemistry of group 12 complexes supported by tetradentate tripodal ligands having internal hydrogen bond donors. *Eur. J. Inorg. Chem*., 273–283.
3. Wada, A., S. Yamaguchi, K. Jitsukawa, and H. Masuda, 2005. Preparation of a hydroperoxo zinc(II) intermediate. *Angew. Chem. Int. Ed*., **44**, 5698–5701.

4. Mareque-Rivas, J. C., R. Prabaharan, and R. T. M. de Rosales, 2004. Relative importance of hydrogen bonding and coordinating groups in modulating zinc-water acidity. *Chem. Commun.*, 76–77.
5. Arii, H., Y. Funahashi, K. Jitsukawa, and H. Masuda, 2003. Preparation and structural characterization of a novel dicoper(II) complex with a terminal hydroxide: A structural model of an active site in phosphohydrolases. *Dalton Trans.*, 2115–2116.
6. Yamaguchi, S., A. Wada, Y. Funahashi, S. Nagatomo, T. Kitagawa, K. Jitsukawa, and H. Masuda, 2003. Thermal stability and absorption spectroscopic behavior of (μ-peroxo)dicopper complexes regulated with intramolecular hydrogen bonding interactions. *Eur. J. Inorg. Chem.*, 4378–4386.
7. Yamaguchi, S., S. Nagatomo, T. Kitagawa, Y. Funahashi, T. Ozawa, K. Jitsukawa, and H. Masuda, 2003. Copper hydroperoxo species activated by hydrogen bonding interaction with its distal oxygen. *Inorg. Chem.*, **42**, 6968–6970.
8. Yamaguchi, S., I. Tokairin, Y. Wakita, Y. Funahashi, K. Jitsukawa, and H. Masuda, 2003. Preparation and characterization of hydroxo-zinc(II) complex surrounded with hydrogen bonding and hydrophobic interaction groups. A structural/functional model of carbonic anhydrases. *Chem. Lett.*, **32**, 406–407.
9. Ogo, S., R. Yamahara, M. Roach, T. Suenobu, M. Aki, T. Ogura, T. Kitagawa, H. Masuda, S. Fukuzumi, and Y. Watanabe, 2002. Structural and spectroscopic features of a *cis* (hydroxo)-Fe(III)-(carboxylato) configuration as an active site model for lipoxygenases. *Inorg. Chem.*, **41**, 5513–5520.
10. Wada, A., S. Ogo, Y. Watanabe, M. Mukai, T. Kitagawa, K. Jitsukawa, H. Masuda, and H. Einaga, 1999. Synthesis and characterization of novel alkylperoxo mononuclear iron(III) complexes with a tripodal pyridylamine ligand: A model for peroxo intermediates in reactions catalyzed by non-heme iron enzymes. *Inorg. Chem.*, **38**, 3592–3593.
11. Wada, A., S. Ogo, S. Nagatomo, T. Kitagawa, Y. Watanabe, K. Jitsukawa, and H. Masuda, 2002. Reactivity of hydroperoxide bound to a mononuclear non-heme iron site. *Inorg. Chem.*, **41**, 616–618.
12. Jitsukawa, K., M. Harata, H. Arii, H. Sakurai, and H. Masuda, 2001. SOD activities of the copper complexes with tripodal polypyridylamine ligands having a hydrogen bonding site. *Inorg. Chim. Acta.*, **324**, 108–116.
13. Ogo, S., S. Wada, Y. Watanabe, M. Iwase, A. Wada, M. Harata, K. Jitsukawa, H. Masuda, and H. Einaga, 1998. Synthesis, structure, and spectroscopic properties of $[Fe^{III}(tnpa)(OH)(PhCOO)]ClO_4$: A model complex for an active form of soybean lipoxygenase-1. *Angew. Chem. Int. Ed. Engl.*, **37**, 2102–2104.

14. Wada, A., M. Harata, K. Hasegawa, K. Jitsukawa, H. Masuda, M. Mukai, T. Kitagawa, and H. Einaga, 1998. Structural and spectroscopic characterization of a mononuclear hydroperoxo-copper(II) complex with tripodal pyridylamine ligands. *Angew. Chem. Int. Ed. Engl.*, **37**, 798–799.
15. Harata, M., K. Hasegawa, K. Jitsukawa, H. Masuda, and H. Einaga, 1998. Preparations, structures, and properties of copper(II) complexes with a new tripodal tetradentate ligand, *N*-(2-pyridylmethyl)bis(6-pivaloylamido-2-pyridylmethyl)amine, and reactivities of the Cu(I) complex with dioxygen. *Bull. Chem. Soc. Jpn.*, **71**, 1031–1038.
16. Harata, M., K. Jitsukawa, H. Masuda, and H. Einaga, 1998. Preparations, structures, and properties of Cu(II) complexes with tripodal tetradentate ligand, tris(6-pivaloylamino-2-pyridylmethyl)amine (htppa), and reaction of its Cu(I) complex with dioxygen. *Bull. Chem. Soc. Jpn.*, **71**, 637–645.
17. Berreau, L. M., S. Mahapatra, J. A. Halfen, V. G. Young, Jr., and W. B. Tolman, 1996. Independent synthesis and structural characterization of a mononuclear copper-hydroxide complex previously assigned as a copper-superoxide species. *Inorg. Chem.*, **35**, 6339–6342.
18. Pascher, T., B. G. Karlsson, M. Nordling, B. G. Malmstrom, and T. Vanngard, 1993. Reduction potentials and their pH dependence in site-directed-mutant forms of azurin from *Pseudomonas aeruginosa*. *Eur. J. Biochem.*, **212**, 289–296.
19. Parks, J. E., B. E. Wagner, and R. H. Holm, 1971. Three-dimensional macrocyclic encapsulation reactions. II. Synthesis and properties of nonoctahedral clathro chelates derived from tris(2-aldoximo-6-pyridyl)phosphine and boron trifluoride or tetrafluoroborate. *Inorg. Chem.*, **10**, 2472–2478.
20. Mandon, D., A. Nopper, T. Litrol, and S. Goetz, 2001. Tridentate coordination of monosubstituted derivatives of the tris(2-pyridylmethyl)amine ligand to $FeCl_3$: Structures and spectroscopic properties of [((2-bromopyridyl)methyl)bis-(2-pyridylmethyl)]amine $Fe^{III}Cl_3$ and [(((2-*p*-methoxyphenyl)pyridyl)methyl)bis(2-pyridylmethyl)]amine $Fe^{III}Cl_3$ and comparison with the [bis(2-pyridylmethyl)]amine $Fe^{III}Cl_3$ complex. *Inorg. Chem.*, **40**, 4803–4806.
21. Chuang, C., K. Lim, Q. Chen, J. Zubieta, and J. W. Canary, 1995. Synthesis, cyclic voltammetry, and X-ray crystal structures of copper(I) and copper(II) complexes of tris((6-phenyl-2-pyridyl)methyl)amine (TPPA). *Inorg. Chem.*, **34**, 2562–2568.
22. Makowska-Grzyska, M. M., E. Szajna, C. Shipley, A. M. Arif, M. H. Mitchell, J. A. Halfen, and L. M. Berreau, 2003. First row divalent transition metal complexes of aryl-appended tris((pyridyl)methyl)amine ligands: Syntheses, structures, electrochemistry, and hydroxamate binding properties. *Inorg. Chem.*, **42**, 7472–7488.

23. Jensen, M. P., S. J. Lange, M. P. Mehn, E. L. Que, and L. Que, Jr., 2003. Biomimetic aryl hydroxylation derived from alkyl hydroperoxide at a nonheme iron center. Evidence for an Fe(IV)=O oxidant. *J. Am. Chem. Soc.*, **125**, 2113–2128.
24. Machkour, A., N. K. Thallaj, L. Benhamou, M. Lachkar, and D. Mandon, 2006. The coordination chemistry of $FeCl_3$ and $FeCl_2$ to bis[2-(2,3-dihydroxyphenyl)-6-pyridylmethyl](2-pyridylmethyl)amine: Access to a diiron(III) compound with an unusual petagonal-bipyramidal/square pyramidal environment. *Chem. Eur. J.*, **12**, 6660–6668.
25. Thallaj, N. K., A. Machkour, D. Mandon, and R. Welter, 2005. Square pyramidal geometry around the metal and tridentate coordination mode of the tripod in the [6-(3′-cyanophenyl)-2-pyridylmethyl]bis(2-pyridylmethyl)amine $FeCl_2$ Complex: A solid state effect. *New J. Chem.*, **29**, 1555–1558.
26. Canary, J. W., C. S. Allen, J. M. Castagnetto, Y.-H. Chiu, P. J. Toscano, and Y. Wang, 1998. Solid state and solution characterization of chiral, conformationally mobile tripodal ligands. *Inorg. Chem.*, **37**, 6255–6262.
27. Chuang, C.-L., K. Lim, and J. W. Canary, 1995. The influence of phenyl substituents on the redox potentials of sterically hindered tripodal ligand/copper complexes. *Supramolecular Chemistry.*, **5**, 39–43.
28. He, Z., D. C. Craig, and S. B. Colbran, 2002. Structures and properties of 6-aryl substituted tris(2-pyridylmethyl)amine transition metal complexes. *J. Chem. Soc., Dalton Trans.*, 4224–4235.
29. Chuang, C.-L., O. dos Santos, X. Xu, and J. W. Canary, 1997. Synthesis and cyclic voltammetry studies of copper complexes of bromo- and alkoxyphenyl-substituted derivatives of tris(2-pyridylmethyl)amine: Influence of cation-alkoxy interactions on copper redox potentials. *Inorg. Chem.*, **36**, 1967–1972.
30. Rudzka, K., M. M. Makowska-Grzyska, E. Szajna, A. M. Arif, and L. M. Berreau, 2005. Neutral acetohydroxamic acid coordination to a mononuclear Ni(II) center stabilized by an intramolecular hydrogen-bonding interaction. *Chem. Commun.*, 489–491.
31. Rudzka, K., A. M. Arif, and L. M. Berreau, 2005. Chemistry of a Ni(II) acetohydroxamic acid complex: Formation, reactivity with water, and attempted preparation of zinc and cobalt analogues. *Inorg. Chem.*, **44**, 7234–7242.
32. Zhu, L., O. dos Santos, C. W. Koo, M. Rybstein, L. Pape, and J. W. Canary, 2003. Geometry-dependent phosphodiester hydrolysis catalyzed by binuclear copper complexes. *Inorg. Chem.*, **42**, 7912–7920.
33. Gross, F. and H. Vahrenkamp, 2005. Zinc complex chemistry of N,N,O ligands providing a hydrophobic cavity. *Inorg. Chem.*, **44**, 3321–3329.

34. Mandon, D., A. Machkour, S. Goetz, and R. Welter, 2002. Trigonal bipyramidal geometry and tridentate coordination mode of the tripod in $FeCl_2$ complexes with tris(2-pyridylmethyl)amine derivatives bis-α-substituted with bulky groups. Structures and spectroscopic comparative studies. *Inorg. Chem.*, **41**, 5364–5372.
35. Lange, S. J., H. Miyake, and L. Que, Jr., 1999. Evidence for a nonheme Fe(IV)=O species in the intramolecular hydroxylation of a phenyl moiety. *J. Am. Chem.*, **121**, 6330–6331.
36. Szajna, E., P. Dobrowolski, A. L. Fuller, A. M. Arif, and L. M. Berreau, 2004. NMR studies of mononuclear octahedral Ni(II) complexes supported by tris((2-pyridyl)methyl)amine-type ligands. *Inorg. Chem.*, **43**, 3988–3997.
37. Jensen, M. P., E. L. Que, X. Shan, E. Rybak-Akimova, and L. Que, Jr. 2006. Spectroscopic and kinetic studies of the reaction of $[Cu^{I}(6\text{-PhTPA})]^{+}$ with O_2. *Dalton Trans.*, 3523–3527.
38. He, Z., S. B. Colbran, and D. C. Craig, 2003. Could redox-switched binding of a redox-active ligand to a copper(II) centre drive a conformational proton pump gate? A synthetic model study. *Chem. Eur. J.*, **9**, 116–129.
39. Xu, X., K. J. Maresca, D. Das, S. Zahn, J. Zubieta, and J. W. Canary, 2002. Crystal-driven distortion of ligands in copper coordination complexes: Conformational pseudo-enantiomers. *Chem. Eur. J.*, **8**, 5679–5683.
40. Nishio, M., Y. Umezawa, M. Hirota, and Y. Takeuchi, 1995. The CH/π interaction: Significance in molecular recognition. *Tetrahedron.*, **51**, 8665–8701.
41. Nishio, M., M. Hirota, and Y. Umezawa, 1998. *The CH/π Interaction: Evidence, Nature and Consequences*, Wiley-VCH, New York.
42. Huheey, J. E., E. A. Keiter, and R. L. Keiter, 1993. *Inorganic Chemistry: Principles of Structure and Reactivity*, 4th ed., HarperCollins College Publishers, New York.
43. Addison, A. W., T. N. Rao, J. Reedijk, J. van Rijn, and G. C. Verschoor, 1984. Synthesis, structure, and spectroscopic properties of copper(II) compounds containing nitrogen-sulfur donor ligands; the crystal and molecular structure of aqua[1,7-bis(*N*-methylbenzimidazol-2′-yl)-2,6-dithiaheptane]-copper(II) perchlorate. *J. Chem. Soc., Dalton Trans.*, 1349–1356.
44. Diebold, A. and K. S. Hagen, 1998. Iron(II) polyamine chemistry: Variation of spin state and coordination number in solid state and solution with iron(II) tris(2-pyridylmethyl)amine complexes. *Inorg. Chem.*, **37**, 215–223.
45. Gütlich, P. 1981. Spin crossover in iron complexes. *Struct. Bonding.*, **44**, 83.
46. Gütlich, P., Y. Garcia, and H. A. Goodwin, 2000. Spin crossover phenomena in Fe(II) complexes. *Chem. Soc. Rev.*, **29**, 419–427.
47. Toftlund, H. 1989. Spin equilibria in iron(II) complexes. *Coord. Chem. Rev.*, **94**, 67–108.

48. Jolly, W. L. 1970. *The Synthesis and Characterization of Inorganic Compounds*, Waveland Press, Prospect Heights, IL.
49. Lever, A. B. P. 1984. *Inorganic Electronic Spectroscopy*, 2nd ed., Elsevier, Amsterdam.
50. Evans, D. F. 1959. The determination of the paramagnetic susceptibility of substances in solution by nuclear magnetic resonance. *J. Chem. Soc.*, 2003–2005.
51. Szajna, E., A. M. Arif, and L. M. Berreau, 2005. Aliphatic carbon-carbon bond cleavage reactivity of a mononuclear Ni(II) cis-β-keto-enolate complex in the presence of base and O_2: A model reaction for acireductone dioxygenase (ARD). *J. Am. Chem. Soc.*, **127**, 17186–17187.
52. Szajna-Fuller, E., K. Rudzka, A. M. Arif, and L. M. Berreau, 2007. Acireductone dioxygenase (ARD)-type reactivity of a Ni(II) Complex having monoanionic coordination of a model substrate: Product identification and comparisons to unreactive analogues. *Inorg. Chem.*, **46**, 5499–5507.
53. Szajna-Fuller, E., B. M. Chambers, A. M. Arif, and L. M. Berreau, 2007. Carboxylate coordination chemistry of a mononuclear Ni(II) center in a hydrophobic or hydrogen bond donor secondary environment: Relevance to acireductone dioxygenases. *Inorg. Chem.*, **46**, 5486–5498.
54. Rudzka, K., A. M. Arif, and L. M. Berreau, 2006. Glyoxalase I-type hemithioacetal isomerization reactivity of a mononuclear Ni(II) deprotonated amide complex. *J. Am. Chem. Soc.*, **128**, 17018–17023.
55. Pavon, J. A. and P. F. Fitzpatrick, 2006. Insights into the catalytic mechanisms of phenylalanine and tryptophan hydroxylase from kinetic isotope effects on aromatic hydroxylation. *Biochemistry*, **45**, 11030–11037.
56. Fitzpatrick, P. F. 2003. Mechanism of aromatic amino acid hydroxylation. *Biochemistry*, **42**, 14083–14091.
57. Fitzpatrick, P. F. 2000. The aromatic amino acid hydroxylases. *Adv Enzymol Relat Areas Mol Biol.*, **74**, 235–294.
58. Moran, G. R., A. Derecskei-Kovacs, P. J. Hillas, and P. F. Fitzpatrick, 2000. On the catalytic mechanism of tryptophan hydroxylase. *J. Am. Chem. Soc.*, **122**, 4535–4541.
59. Fitzpatrick, P. F. 1999. Tetrahydropterin-dependent amino acid hydroxylases. *Annu. Rev. Biochem.*, **68**, 355–381.
60. Goodwill, K. E., C. Sabatier, C. Marks, R. Raag, P. F. Fitzpatrick, and R. C. Stevens, 1997. Crystal structure of tyrosine hydroxylase at 2.3 Å and its implications for inherited neurodegenerative diseases. *Nat. Struct. Biol.*, **4**, 578–585.
61. Flatmark, T. and R. C. Stevens, 1999. Structural insight into the aromatic amino acid hydroxylases and their disease-related mutant forms. *Chem. Rev.*, **99**, 2137–2160.

62. Hillas, P. J. and P. F. Fitzpatrick, 1996. A mechanism for hydroxylation by tyrosine hydroxylase based on partitioning of substituted phenylalanines. *Biochemistry*, **35**, 6969–6975.
63. Kappock, T. J. and J. P. Caradonna, 1996. Pterin-dependent amino acid hydroxylases. *Chem. Rev.*, **96**, 2659–2756.
64. Frantom, P. A., R. Pongdee, G. A. Sulikowksi, and P. F. Fitzpatrick, 2002. Intrinsic deuterium isotope effects on benzylic hydroxylation by tyrosine hydroxylase. *J. Am. Chem. Soc.*, **124**, 4202–4203.
65. Jensen, M. P., M. P. Mehn, and L. Que, Jr., 2003. Intramolecular aromatic amination through iron-mediated nitrene transfer. *Angew. Chem. Int. Ed.*, **42**, 4357–4360.
66. Solomon, E. I., U. M. Sundaram, and T. E. Machonkin, 1996. Multicopper oxidases and oxygenases. *Chem. Rev.*, **96**, 2563–2606.
67. Tolman, W. B. 2006. Using synthetic chemistry to understand copper protein active sites: A personal perspective. *J. Biol. Inorg. Chem.*, **11**, 261–271.
68. Mirica, L. M., D. J. Rudd, M. A. Vance, E. I. Solomon, K. O. Hodgson, B. Hedman, and T. D. P. Stack, 2006. μ-η^2:η^2-Peroxodicopper(II) complex with a secondary diamine ligand: A functional model of tyrosinase. *J. Am. Chem. Soc.*, **128**, 2654–2665.
69. Mirica, L. V., M. Vance, D. J. Rudd, B. Hedman, K. O. Hodgson, E. I. Solomon, and T. D. P. Stack, 2005. Tyrosinase reactivity in a model complex: An alternative hydroxylation mechanism. *Science*, **308**, 1890–1892.
70. Lewis, E. A. and W. B. Tolman, 2004. Reactivity of dioxygen-copper systems. *Chem. Rev.*, **104**, 1047–1076.
71. Palavicini, S., A. Granata, E. Monzani, and L. Casella, 2005. Hydroxylation of phenolic compounds by a peroxodicopper(II) complex: Further insight into the mechanism of tyrosinase. *J. Am. Chem. Soc.*, **127**, 18031–18036.
72. Itoh, S. 2004. In *Comprehensive Coordination Chemistry II*, McCleverty, J. A. and T. J. Meyer (eds.), vol. 8, pp. 369–393, Elsevier, Amsterdam.
73. Hatcher, L. Q. and K. D. Karlin, 2004. Oxidant types in copper-dioxygen chemistry: The ligand coordination defines the Cu(n)-O_2 structure and subsequent reactivity. *J. Biol. Inorg. Chem.*, **9**, 669–683.
74. Mirica, L. M., M. Vance, D. J. Rudd, B. Hedman, K. O. Hodgson, E. I. Solomon, and T. D. P. Stack, 2002. A stabilized μ-η^2:η^2-peroxodicopper(II) complex with a secondary diamine ligand and its tyrosinase-like reactivity. *J. Am. Chem. Soc.*, **124**, 9332–9333.
75. Pidcock, E., H. V. Obias, C. X. Zhang, K. D. Karlin, and E. I. Solomon, 1998. Investigation of the reactive oxygen intermediate in an arene hydroxylation reaction performed by xylyl-bridged binuclear copper complexes. *J. Am. Chem. Soc.*, **120**, 7841–7847.

76. Holland, P. L., K. R. Rogers, and W. B. Tolman, 1999. Is the bis(μ-oxo)dicopper core capable of hydroxylating an arene? *Angew. Chem. Int. Ed.*, **38**, 1139–1142.
77. Wray, J. W. and R. H. Abeles, 1993. A bacterial enzyme that catalyzes the formation of carbon monoxide. *J. Biol. Chem.*, **268**, 21466–21469.
78. Myers, R. W., J. W. Wray, S. Fish, and R. H. Abeles, 1993. Purification and characterization of an enzyme involved in oxidative carbon-carbon bond cleavage reactions in the methionine salvage pathway of *Klebsiella pneumoniae. J. Biol. Chem.*, **268**, 24785–24791.
79. Wray, J. W. and R. H. Abeles, 1995. The methionine salvage pathway in *Klebsiella pneumoniae* and rat liver. Identification and characterization of two novel dioxygenases. *J. Biol. Chem.*, **270**, 3147–3153.
80. Dai, Y., P. C. Wensink, and R. H. Abeles, 1999. One protein, two enzymes. *J. Biol. Chem.*, **274**, 1193–1195.
81. Dai, Y., T. C. Pochapsky, and R. H. Abeles, 2001. Mechanistic studies of two dioxygenases in the methionine salvage pathway of *Klebsiella pneumoniae. Biochemistry*, **40**, 6379–6387.
82. Al-Mjeni, F., T. Ju, T. C. Pochapsky, and M. J. Maroney, 2002. XAS investigation of the structure and function of Ni in acireductone dioxygenase. *Biochemistry*, **41**, 6761–6769.
83. Pochapsky, T. C., S. S. Pochapsky, T. Ju, H. Mo, F. Al-Mjeni, and M. J. Maroney, 2002. Modeling and experiment yields the structure of acireductone dioxygenase from *Klebsiella pneumoniae. Nat. Struct. Biol.*, **9**, 966–972.
84. Pochapsky, T. C., S. S. Pochapsky, T. Ju, C. Hoefler, and J. Liang, 2006. A refined model for the structure of acireductone dioxygenase from *Klebsiella ATCC 8724* incorporating residual dipolar couplings. *J. Biomol. NMR.*, **34**, 117–127.
85. Ju, T., R. B. Goldsmith, S. C. Chai, M. J. Maroney, S. S. Pochapsky, and T. C. Pochapsky, 2006. One protein, two enzymes revisited: A structural entropy switch interconverts the two isoforms of acireductone dioxygenase. *J. Mol. Biol.*, **363**, 823–834.
86. Pochapsky, T. C., T. Ju, M. Dang, R. Beaulieu, G. M. Pagini, and B. OuYang, 2007. In *Nickel and Its Surprising Impact in Nature: Metal Ions in Life Sciences*, Sigel, A., H. Sigel, and R. K. O. Sigel (eds.), vol. 2, Wiley, Chichester, UK.
87. Marmion, C. J., D. Griffith, and K. B. Nolan, 2004. Hydroxamic acids—an intriguing family of enzyme inhibitors and biomedical ligands. *Eur. J. Inorg. Chem.*, 3003–3016.
88. Dixon, N. E., C. Gazzola, J. J. Watters, R. l. Blakeley, and B. Zerner, 1975. Inhibition of jack bean urease (EC 3.5.1.5) by acetohydroxamic acid and by phosphoramidate. Equivalent weight for urease. *J. Am. Chem. Soc.*, **97**, 4130–4131.

89. Dixon, N. E., J. A. Hinds, A. K. Fihelly, C. Gazzola, D. J. Winzor, R. L. Blakeley, and B. Zerner, 1980. Jack bean urease (EC 3.5.1.5). IV. The molecular size and the mechanism of inhibition by hydroxamic acids. Spectrophotometric titration of enzymes with reversible inhibitors. *Can. J. Biochem.*, **58**, 1323–1334.
90. Mobley, H. L. T. and R. P. Hausinger, 1989. Microbial ureases: Significance, regulation, and molecular characterization. *Microbiol. Rev.*, **53**, 85–108.
91. Mobley, H. L. T., M. D. Island, and R. P. Hausinger, 1995. Molecular biology of microbial ureases. *Microbiol. Rev.*, **59**, 451–480.
92. Todd, M. J. and R. P. Hausinger, 1989. Competitive inhibitors of *Klebsiella aerogenes* urease. Mechanisms of interaction with the nickel active site. *J. Biol. Chem.*, **264**, 15835–15842.
93. Pearson, M. A., L. O. Michel, R. P. Hausinger, and P. A. Karplus, 1997. Structures of cys_{319} variants and acetohydroxamate-inhibited *Klebsiella aerogenes* urease. *Biochemistry*, **36**, 8164–8172.
94. Benini, S., W. R. Rypniewski, K. S. Wilson, S. Miletti, S. Ciurli, and S. Mangani, 2000. The complex of *Bacillus pasteurii* urease with acetohydroxamate anion from X-ray data at 1.55 Å resolution. *J. Biol. Inorg. Chem.*, **5**, 110–118.
95. Stemmler, A. J., J. W. Kampf, M. L. Kirk, and V. L. Pecoraro, 1995. A model for the inhibition of urease by hydroxamates. *J. Am. Chem. Soc.*, **117**, 6368–6369.
96. Arnold, M., D. A. Brown, O. Deeg, W. Errington, W. Haase, K. Herlihy, T. J. Kemp, H. Nimir, and R. Werner, 1998. Hydroxamate-bridged dinuclear nickel complexes as models for urease inhibition. *Inorg. Chem.*, **37**, 2920–2925.
97. Thornalley, P. J. 1990. The glyoxalase system: New developments towards functional characterization of a metabolic pathway fundamental to biological life. *Biochem. J.*, **269**, 1–11.
98. Clugston, S. L., J. F. J. Barnard, R. Kinach, D. Miedema, R. Ruman, E. Daub, and J. F. Honek, 1998. Overproduction and characterization of a dimeric non-zinc glyoxalase I from *Escherichia coli*: Evidence for optimal activation by nickel ions. *Biochemistry*, **37**, 8754–8763.
99. Clugston, S. L., R. Yajima, and J. F. Honek, 2004. Investigation of metal binding and activation of *Escherichia coli* glyoxalase I: Kinetic, thermodynamic and mutagenesis studies. *Biochem. J.*, **377**, 309–316.
100. Vickers, T. J., N. Greig, and A. H. Fairlamb, 2004. A trypanothione-dependent glyoxalase I with a prokaryotic ancestry in *Leishmania major*. *Proc. Natl. Acad. Sci.*, **101**, 13186–13191.
101. He, M. M., S. L. Clugston, J. F. Honek, and B. W. Matthews, 2000. Determination of the structure of *Escherichia coli* glyoxalase I suggests a

structural basis for differential metal activation. *Biochemistry*, **39**, 8719–8727.

102. Klinker, E. J., T. A. Jackson, M. P. Jensen, A. Stubna, G. Juhasz, E. L. Bominaar, E. Munck, and L. Que, Jr., 2006. A tosylimido analogue of a nonheme oxoiron(IV) complex. *Angew. Chem. Int. Ed.*, **45**, 7394–7397.
103. Straganz, G. D. and B. Nidetzky, 2006. Variations of the 2-his-1-carboxylate theme in mononuclear non-heme Fe^{II} oxygenases. *Chembiochem.*, **7**, 1536–1548.
104. Dunwell, J. M., A. Purvis, and S. Khuri, 2004. Cupins: The most functionally diverse protein superfamily? *Phytochemistry*, **65**, 7–17.
105. Dunwell, J. M., A. Culham, C. E. Carter, C. R. Sosa-Aguirre, and P. W. Goodenough, 2001. Evolution of functional diversity in the cupin superfamily. *Trends Biochem. Sci.*, **26**, 740–746.
106. Reinhardt, L. A., D. Svedruzic, C. H. Chang, W. W. Cleland, and N. G. J. Richards, 2003. Heavy atom isotope effects on the reaction catalyzed by the oxalate decarboxylase from *Bacillus subtilis*. *J. Am. Chem. Soc.*, **125**, 1244–1252.
107. Zhang, Y., M. H. Heinsen, M. Kostic, G. M. Pagani, T. V. Riera, I. Perovic, L. Hedstrom, B. B. Snider, and T. C. Pochapsky, 2004. Analogs of 1-phosphonooxy-2,2-dihydroxy-3-oxo-5-(methylthio)pentane, an acyclic intermediate in the methionine salvage pathway: A new preparation and characterization of activity with E1 enolase/phosphatase from *Klebsiella oxytoca*. *Bioorg. Med. Chem.*, **12**, 3847–3855.
108. Fuller, A. L. 2005. MS Thesis, Utah State University.
109. Fuller, A. L., R. W. Watkins, K. R. Dunbar, A. V. Prosvirin, A. M. Arif, and L. M. Berreau, 2005. Manganese(II) chemistry of a new N_3O-donor chelate ligand: Synthesis, X-ray structures and magnetic properties of solvent- and oxalate-bound complexes. *Dalton Trans.*, 1891–1896.
110. Glerup, J., P. A. Goodson, D. J. Hodgson, and K. Michelsen, 1995. Magnetic exchange through oxalate bridges: Synthesis and characterization of (μ-oxalato)dimetal(II) complexes of manganese, iron, cobalt, nickel, copper, and zinc. *Inorg. Chem.*, **34**, 6255–6264.